



# STAR

(Contract Number:Fission-2010-3.5.1-269672)

## DELIVERABLE (D-N°5.4)

### Understanding the “metabolic” mode of actions of two different types of radiation using biokinetics/DEB-tox models

**Authors:** Frédéric Alonzo, Elke Zimmer, Delphine Plaire, Adeline Buisset-Goussen, Christelle Adam-Guillermin, Catherine Lecomte-Pradines, Nele Horemans

**Editors:** Nele Horemans, Frédéric Alonzo, Elke Zimmer, Thomas Hinton

Reporting period: 01/08/2012 - 20/08/2014

Report issued: 20/08/2014

Start date of project: 01/02/2011

Duration: 54 Months

## DISTRIBUTION LIST

Name	Number of copies	Comments
André Jouve, STAR EC Project Officer	1	Electronically
Thomas Hinton, STAR Co-ordinator WP-1, IRSN	1	Electronically (pdf file)
Laureline Février, Assistant Co-ordinator IRSN	1	Electronically (pdf file)
STAR Management Team members: WP-2; T. Ikaheimonen, STUK WP-3; A. Liland, NRPA WP-4; H. Vandenhove, SCK•CEN WP-5; F. Alonzo, IRSN WP-6; D. Oughton, NMBU WP-7; B. Howard, NERC	1 per member	Electronically (pdf file)
STAR Steering Committee M. Steiner, BfS A. Real, CIEMAT J-C. Gariel, IRSN T. Ikaheimonen, STUK H. Vandenhove, SCK•CEN C. Bradshaw, SU A. Liland, NRPA B. Howard, NERC B. Salbu, NMBU	1 per member	Electronically (pdf file)
STAR Wiki site		
STAR's External Advisory Board		Electronically (pdf file)
Radioecology Alliance members	1 per member	Electronically (pdf file)
	1 per member	Electronically (pdf file)

Project co-funded by the European Commission under the Seventh Euratom Framework Programme for Nuclear Research & Training Activities (2007-2011)		
Dissemination Level		
<b>PU</b>	Public	PU
<b>RE</b>	Restricted to a group specified by the partners of the [STAR] project	
<b>CO</b>	Confidential, only for partners of the [STAR] project	

## List of Acronyms and Abbreviations

AIC: Akaike Information Criteria

Radioecology Alliance (European Radioecological Alliance association): A Research Platform, in accordance with relevant European Union policies which coordinate and promote European research on radioecology

DBS: Double Strand Breaks

DEB(tox): Dynamic Energy Budget model

DEB-tox: model of dynamic energy budget applied to toxicology

DoW: Description of Work

DR: dose rate

EC: European Commission

EC<sub>x</sub>: concentration of a compound giving x% effect

ERICA: Environmental Risk from Ionising Contaminants: Assessment and Management

FASSET: Framework for Assessment of Environmental Impact

FREDERICA: Radiation Effects Database based on two EC-projects FASSET and EPIC (Environmental Protection of Ionising Contaminants in the Arctic)

HR: Homologous Recombination

LET: Linear Energy Transfer

NEC or NEC<sub>1</sub>: no-effect concentration

NEC<sub>2</sub>: no-damage concentration

NEDR: no-effect dose rate

NHEJ: Non-Homologous End-Joining

OECD: Organisation of Economic Cooperation and Development

RAPD-qPCR: randomly amplified polymorphic DNA by quantitative polymerase chain reaction

RBE: Relative Biological Effectiveness

ROS: Reactive Oxygen Species

STAR (Strategy for Allied Radioecology): An EC-funded Network of Excellence in radioecology under the Radioecology Alliance framework

SSQ: Sum of Squares

WP: Work Package

## Table of Contents

List of Acronyms and Abbreviations .....	3
1 Summary .....	6
2 Introduction .....	7
2.1 Background.....	7
2.1.1 Mathematical models in ecological risk assessment.....	7
2.1.2 Elements of energy budget theory (DEB).....	8
2.1.3 A simplified DEB-tox approach for animals.....	10
2.1.4 The differences between animal and plant DEB models .....	14
2.2 Dependency of radiological stress on dose rate.....	15
2.3 Modes of action associated with radiotoxicity: molecular and cellular mechanisms and their consequences for energy budget .....	16
2.4 Analysis of relative biological effectiveness: a mechanistic comparison of toxicity between alpha and gamma radiation .....	19
3 <i>Caenorhabditis elegans</i> .....	20
3.1 Background.....	20
3.2 Formulation of a DEB-tox model applied to chronic external gamma radiation ....	20
3.2.1 Model assumptions.....	20
3.2.2 Parameterization.....	24
3.2.3 Results .....	26
4 <i>Daphnia magna</i> .....	33
4.1 Introduction.....	33
4.2 DEB-tox applied to a multigenerational depleted uranium exposure.....	33
4.2.1 Background .....	33
4.2.2 Formulation of a dual-stress DEB-tox model .....	34
4.2.3 Parameterization.....	40
4.2.4 Results .....	41
4.3 Mechanistic comparison of gamma and alpha effects: identifying modes of actions and quantifying RBE.....	53
4.3.1 Background .....	53
4.3.2 Future directions.....	53

5	<i>Lemna minor</i> .....	56
5.1	Introduction.....	56
5.2	The simplest DEB model for <i>Lemna minor</i> .....	57
5.2.1	Purpose of the model.....	57
5.2.2	Modelling approach / Assumptions.....	57
5.2.3	Possible extensions.....	59
5.3	Data needs for parameterization and verification .....	61
5.4	Effect of light, temperature and growth medium on <i>L. minor</i> growth, Uranium as a case study .....	62
5.5	Gamma.....	62
6	General conclusions and perspectives.....	64
7	References .....	66

# 1 Summary

Understanding how toxic contaminants affect wildlife species at various levels of biological organisation (sub-cellular, histological, physiological, organism, population levels) is a major research goal in both ecotoxicology and radioecology. A mechanistic understanding of the links between the different observed perturbations is necessary to predict consequences for survival, growth and reproduction which are critical for population dynamics. However, time scales at which such links are established in the laboratory are rarely relevant for natural populations. Multigenerational exposures are much more representative of the real context of field populations for which exposure can last for durations which largely exceed individual longevity and involve exposure of many successive generations. In this context, STAR conducted both experimental and modelling studies under controlled conditions in three model species: two animals: the nematode *Caenorhabditis elegans* and the cladoceran microcrustacean *Daphnia magna* and one plant the macrophyte *Lemna minor*.

In *C. elegans*, a chronic external gamma exposure was conducted as part of STAR WP5 pilot study (Lecomte-Pradines *et al.*, in preparation). In *D. magna*, multigenerational investigations of toxic effects on survival, somatic growth and reproduction were achieved for various radioactive substances including depleted uranium (U-depl), americium-241 (Am-241) and cesium-137 (Cs-137), representing respectively dominant chemotoxicity, radiotoxicity through alpha internal contamination and through gamma external irradiation (Alonzo *et al.*, 2008; Massarin *et al.*, 2010; Plaire *et al.*, 2013; Parisot *et al.*, in preparation). Accumulation and transmission of DNA damage were investigated with U-depl and gamma radiation. Finally for *L. minor* a seven day growth inhibition test was used to study the effect of uranium (U), Am-241 and gamma radiation. Due to the low solubility of Am-241 in the different test, *L. minor* growth experiments were not continued. With their small sizes and short life cycles, *C. elegans*, *D. magna* and *L. minor* are particularly suitable test models for exploring how chronic exposure to radioactive substances alter DNA and affect life history traits (survival, growth and reproduction) over several generations. A note has to be taken that for *L. minor* reproduction is predominantly asexually.

The present report describes how reduction in somatic growth and reproduction induced by gamma irradiation in *C. elegans* and U-depl in *D. magna* can be explained using the mechanistic modelling approach known as DEB-tox (model of dynamic energy budget applied to toxicology). Results of DEB-tox analyses suggested that external gamma radiation increases costs for growth and maturation in *C. elegans*, causing the delay observed in growth and reproduction, together with a direct effect on reproduction. U-depl primarily affects assimilation in *D. magna*. However, a model considering the accumulation and transmission of genetic damage is necessary to understand the increase in effects over successive generations. Results suggested the involvement of a second mode of action explaining consequences of cumulated damage across generations. The nature of the second mode of action remains to be confirmed experimentally, whereby DEB-tox analyses are pointing to an increase in costs for growth and maturation. This mode of action needs to be confirmed also in *D. magna* exposed to gamma or alpha radiation for several generations, in a mechanistic

analysis of relative biological effectiveness which takes account of the difference in kinetics of stress between the two types of ionising radiation.

A similar DEB-tox approach was pursued for *L. minor* to enable comparison of mode of action of alpha and gamma radiation between the different species. However, plants and animals differ greatly in the way they accumulate nutrients and therefore the basic DEB model for plants and animals will also be different. As to date no plant DEB model was described, thus the first challenge was to obtain the necessary data and approach to parameterise a DEB model for *L. minor*. Hence, a number of experiments were performed studying the growth of *L. minor* under different conditions such as varying light-intensity, -exposure, and temperature. In addition contact was made with N. Cedergreen (University of Copenhagen) to examine the possibilities to include the vast dataset on *L. minor* that she has in the parameterisation of the DEB model. Together with the exposure data of *L. minor* to U and gamma irradiation, different DEB(tox)models are being tested.

The current report is structured as follows. In the introduction first a general description of DEB-tox concepts is given followed by an in depth mathematical description of the model used for the animal studies and a comparison between animal and plant models. Subsequently the dependency of radiation on dose rate and the possible modes of action of radiation in plants and animals is given. The final part of the introduction touches upon the mechanistic comparison of toxicity between alpha and gamma radiation and whether relative biological effectiveness can be analysed using a DEB-tox approach. The major part of the report contains three sections successively describing the results obtained for *C. elegans*, *D. magna* and *L. minor*. Finally the major conclusions of the work performed in WP5.4 and perspectives for the work within the remaining months of STAR are given. In general, the DEB-tox analysis of the *C. elegans* and *D. magna* experiments show its great potential for comparing effects of different stressors, especially radiation, on different species. However, it also shows the difficulties and uncertainties that still need to be resolved. Although at this moment work especially for *L. minor* is still in progress it was additionally shown that observed effects do differ depending on the dose rate. As such, in *D. magna*, it seems that from a certain dose rate, the effects extend to additional costs on growth or reproduction (see section 4). For *L. minor* it was shown that from a certain dose rate the plants were unable to recover from radiation exposure (see section 5). Although further testing is necessary, there might be a dose rate in between the range we tested in which also first costs for growth are affected. DEB models provide the perfect stage for these types of comparisons between effect patterns and species.

## 2 Introduction

### 2.1 Background

#### 2.1.1 Mathematical models in ecological risk assessment

The need for biology-based mathematical models for ecological risk assessment has been emphasized in deliverable D5.1. In contrast to empirically derived statistical relationships such as the ECX-concentrations, biology-based models allow for extrapolation to non-tested

scenarios as they account for the underlying mechanisms. One biology-based, mechanistic effect modelling framework that has received much attention in the recent past is Dynamic Energy Budget (DEB) theory. Models based on DEB are the basis for so-called DEB-tox models, which can be used for interpreting effects of stressors as effects on general processes such as (i) maintenance, (ii) assimilation, (iii) somatic growth and (iv) reproduction. Effects of stressors are reflected in changes in DEB parameters, which allows for investigating the interaction of multiple stressors, both natural (e.g. temperature, resource availability) and anthropogenic (e.g. toxic chemicals, radiation). DEB models are designed for capturing the energy metabolism of individuals, and can thus be naturally linked with individual-based models for population level assessment (Martin et al, 2011). While DEB-tox models have been used widely in ecotoxicology to interpret effects on animals, DEB-tox has never been applied to a plant. In fact, no DEB model for a plant has been developed and tested until now. The main challenge of applying DEB-tox for *L. minor* thus lies in the development of a basic DEB model for the plant.

### 2.1.2 Elements of energy budget theory (DEB)

In a general way, energy budget models describe how an organism acquires energy from food and use it to support its major biological functions including survival, growth and reproduction. In the literature, the majority of models published for different species can be classified into two types, namely, net production models and net assimilation models. These two types of models differ mainly in hypotheses concerning energy allocation to reproduction (Lika and Nisbet, 2000). In a net production model, organism maintenance, which is critical for survival, is directly deduced from energy acquisition. Thus, growth and reproduction are predicted from the difference between assimilation and respiration (Noonburg et al., 1998; Lika and Nisbet, 2000). In a net assimilation model, energy consumed in respiration reflects expenses associated with the achievement of all biological functions including growth and reproduction. Consequently, growth, reproduction and respiration are predicted from assimilation. DEB models used in this work (Figure 1) are net assimilation models (Kooijman, 2010).

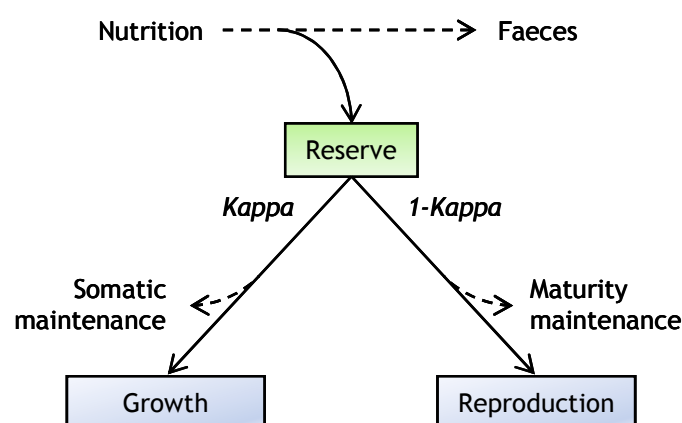


Figure 1: Conceptual diagram of organism metabolism as defined by the DEB theory (Kooijman, 2010)

In the DEB model (Kooijman, 2010), energy acquired from nutrition is stored in a reserve compartment. A constant fraction “*Kappa*” of this reserve is allocated to soma while the remaining fraction (1-*Kappa*) is used to support processes associated with reproduction. In the *Kappa* fraction, energy is first allocated to somatic maintenance, which allows the body structure to survive. The remaining energy in the *Kappa* fraction is then allocated to growth (increase in body structure). In the fraction (1-*Kappa*), energy is first allocated to maturity maintenance. The remaining energy is used in maturation (increase in maturity). Once organisms reach a certain level of maturity (defined as puberty), reproduction starts and the fraction of energy which is not consumed in maintaining maturity is used to produce offspring.

In this theory, life cycles are divided in three major stages, marked by important changes in energy budget:

- the embryonic stage in which organisms do not feed and live using a reserve deposited in eggs;
- the juvenile stage in which organisms feed and allocate their energy to maturation (puberty is not reached);
- the adult stage in which organisms have reached puberty and reproduce.

The model provides differential equations describing the dynamics of the reserve compartment and of energy allocation to growth and reproduction. A change in the *Kappa* fraction occurs only in the presence of toxics or parasites which strongly modify organism functioning.

Under constant conditions (including food density), the reserve density is constant over the life cycle. The DEB model delivers growth and reproduction predictions (Figure 2). Body size increases in time from a length at birth ( $L_b$ ), causing an increase in assimilation (as a function of the square of body length) and a larger increase in somatic maintenance (as a function of the cube of body length). Consequently, body size increases following a Von Bertalanffy law

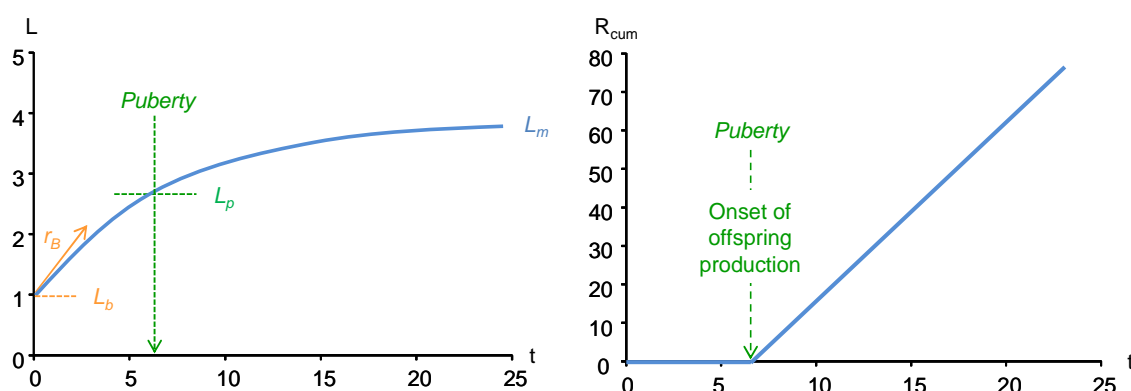


Figure 2 : Theoretical curves of size( $L$ ) and cumulated reproduction ( $R_{cum}$ ) under optimal conditions.  $L_b$ : Size at birth;  $L_p$ : Size at puberty;  $L_m$ : Maximal size;  $r_B$ : von Bertalanffy growth rate.

to a maximum length ( $L_m$ ) reached when the whole  $Kappa$  fraction is used to support costs of somatic maintenance and no more energy is available for growth. After puberty is reached, (when body length reaches  $L_p$  the length at puberty) energy allocation in reproduction shifts from gonad maturation to offspring production.

### 2.1.3 A simplified DEB-tox approach for animals

The Dynamic Energy Budget theory applied to toxicology (DEB-tox) offers many advantages for analyzing and interpreting toxic effects measured on life history traits. In fact, the approach considers effects as dynamic processes. Based on the DEB theory, it establishes links between metabolic perturbations and their consequences on growth, reproduction and survival, which are critical for the population (Nisbet *et al.*, 2000; Jager and Zimmer, 2012). With its capacity to integrate organisms functioning, common ecotoxicological parameters are estimated for the different endpoints. These parameters are independent of exposure duration (unlike NOEC and EC, the classical no-observed effect concentration and the effective concentration affecting a specific endpoint after fixed exposure duration) and exposure concentration (Kooijman and Bedaux, 1996). Recent studies by Swain *et al.* (2010) and Wren *et al.* (2011) suggest coupling DEB-tox approach to effects at the molecular level such as expression of specific gene associated with metabolism in the nematode *Caenorhabditis elegans*.

The DEB-tox model was initially developed by Kooijman and Metz (1984) and Kooijman and Bedaux (1996). A revised formulation was proposed by Billoir *et al.* (2008) and Jager and Zimmer (2012). The simplified DEB-tox model is based on three assumptions which substantially reduce the model complexity. First, it is assumed that maturity is a constant fraction of structure. This means that maturity does not have to be followed as a state variable. It implies that the test organisms reach puberty at a constant size independent of food availability, and that offspring has a constant size at birth. Second, it is assumed that the energetic costs for an egg are always the same, which is in contrast to the standard DEB assumption for 'maternal effects'. The third assumption is that reserve is always in equilibrium with the food level, which is realistic when food availability is constant. All these assumptions usually hold for ecotoxicological tests, but need to be kept in mind when applying the DEB-tox model to a new test organism.

The DEB-tox combines toxicant kinetics and effects dynamics, i.e. the model first describes how a toxic compound is accumulated over time within an exposed organism and second, how this contamination alters processes of the DEB. In this context, a one compartment kinetic model with first order kinetics is used. Toxic intake and elimination are proportional to body surface and, respectively, to exposure concentration  $C_e$  and internal concentration  $C_i$ :

$$\frac{dC_i}{dt} = C_e \frac{k_a}{l} - C_i \left( \frac{k_e}{l} + \frac{d}{dt} \ln l^3 \right)$$

With  $k_a$  and  $k_e$  the surface-specific accumulation and elimination rates (in  $\text{time}^{-1}$ ) and where the term  $\frac{d}{dt} \ln l^3$  corresponds to the dilution of toxicant burden by growth.

In order to reduce the number of parameters in the model, the internal concentration  $C_i$  is scaled by the bioconcentration factor as following:  $C_i^* = \frac{k_e}{k_a} C_i$  with  $C_i^*$  the scaled internal toxicant -concentration (Kooijman and Bedaux, 1996), proportional to the actual but unknown internal concentration  $C_i$  and tending at equilibrium towards the value of exposure concentration  $C_e$ . As gamma irradiation is not taken up or accumulates similar to chemicals a section on the possible implications of this for DEB-tox is given below in section 2.2. Based on the transformation, the toxicant kinetics can be described by the following simplified equation:

$$\frac{dC_i^*}{dt} = C_e \frac{k_e}{l} - C_i^* \left( \frac{k_e}{l} + \frac{d}{dt} \ln l^3 \right)$$

All parameters are represented in the Table 1.

The internalized toxic compound is assumed to affect energy budget (energy intake and/or allocation) through to a stress function  $\sigma$ , when the scaled internal concentration exceeds a

Table 1 : DEB-tox model parameters

Symbol	Unit	Interpretation
$L_m$	mm	Maximum length
$L_b$	mm	Length at birth
$L_p$	mm	Length at puberty
$l$	-	Scaled size by maximum length
$l_b$	-	Scaled length at birth by maximum length
$l_p$	-	Scaled length at puberty by maximum length
$r_B$	$d^{-1}$	von Bertalanffy growth rate
$R_m$	$\mu g \text{ egg } d^{-1}$	Maximum reproduction rate
$R$	$\mu g \text{ egg } d^{-1}$	Daily reproduction rate
$k_a$	$d^{-1}$	Toxicant accumulation rate
$k_e$	$d^{-1}$	Toxicant elimination rate
$k_d$	$d^{-1}$	Damage accumulation rate
$k_r$	$d^{-1}$	Damage reparation rate
$NEC$	$\mu g L^{-1}$	No effect concentration
$b$	$L \mu g^{-1}$	Slope of stress intensity
$C_e$	$\mu g L^{-1}$	Exposure concentration
$C_i$	$\mu g L^{-1}$	Internal concentration
$C_i^*$	$\mu g L^{-1}$	Scaled internal concentration by its bioconcentration factor
$D^*$	$\mu g L^{-1}$	Scaled damages level by its bioconcentration factor
$\sigma$	-	Stress intensity
$g$	-	Energy investment ratio
$f$	-	Scaled nutritional functional response

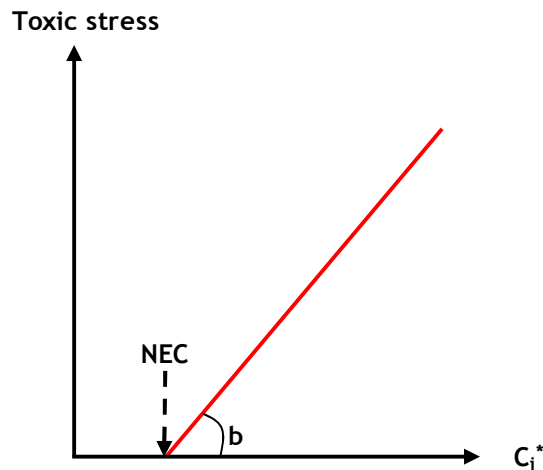


Figure 3 :Stress intensity as a function of internal toxicant concentration (with *NEC*, the no-effect concentration)

threshold value named *NEC* (Figure 3), for no-effect concentration (Kooijman and Bedaux, 1996):

$$\begin{cases} \sigma(C_i^*) = 0 & \text{if } C_i^* < NEC \\ \sigma(C_i^*) = b \cdot (C_i^* - NEC) & \text{if } C_i^* \geq NEC \end{cases}$$

Kooijman and Bedaux (1996) initially suggest five different metabolic modes of action to interpret toxic effects on reproduction. Several other modes of action are added in Kooijman (2010). Various sets of equations initially derived by Kooijman and Bedaux (1996) and revised by (Billoir *et al.*, 2008, are available depending on the considered mode of action (Table 2).

The three first modes of action are indirect modes of action where the contaminant is assumed to affect both growth and reproduction (Billoir *et al.*, 2008):

- The *Growth model* suggests that the internalized toxicant causes increase in costs for growth and maturation, through the term  $1 + \sigma(C_i^*)$ .
- The *Maintenance model* suggests that the internalized toxicant causes an increase in costs for somatic and maturity maintenance, through the term  $1 + \sigma(C_i^*)$ .
- The *Assimilation model* suggests that the internalized toxicant causes a decrease in assimilation, through the term  $1 - \sigma(C_i^*)$ .

The two last modes of action correspond to a direct effect of the contaminant on reproduction, while growth is not affected (Billoir *et al.*, 2008):

- The *Hazard model* suggests that the internalized toxicant causes an increase in mortality during oogenesis, through the term  $\exp(-\sigma(C_i^*))$ .
- The *Cost model* suggests that the internalized toxicant causes an increase in costs for egg production, through the term  $1 + \sigma(C_i^*)$ .

Table 2: Sets of differential equations for growth and reproduction based on a simplified DEB-tox model (assuming constant exposure conditions).

Effect models	Growth	Reproduction
	$l(0) = l_b$	$R(l) = 0 \text{ if } l < l_p$
Growth model	$\frac{dl}{dt} = r_B \frac{f+g}{f+g(1+\sigma(C_i^*))} (f-l)$	$R(l) = \frac{R_m}{1-l_p^3} \left[ f l^2 \left( \frac{g(1+\sigma(C_i^*)) + l}{g(1+\sigma(C_i^*)) + f} \right) - l_p^3 \right]$
Maintenance model	$\frac{dl}{dt} = r_B (f - l(1 + \sigma(C_i^*)))$	$R(l) = \frac{R_m}{1-l_p^3} (1 + \sigma(C_i^*)) \left[ f l^2 \left( \frac{g(1 + \sigma(C_i^*))^{-1} + l}{g + f} \right) - l_p^3 \right]$
Assimilation model	$\frac{dl}{dt} = r_B \frac{f+g}{f(1-\sigma(C_i^*)) + g} (f(1-\sigma(C_i^*)) - l)$	$R(l) = \frac{R_m}{1-l_p^3} \left[ f(1-\sigma(C_i^*)) l^2 \left( \frac{g+l}{g+f(1-\sigma(C_i^*))} \right) - l_p^3 \right]$
Hazard model	$\frac{dl}{dt} = r_B (f - l)$	$R(l) = \frac{R_m}{1-l_p^3} \left[ f l^2 \left( \frac{g+l}{g+f} \right) - l_p^3 \right] e^{-\sigma(C_i^*)}$
Costs model	$\frac{dl}{dt} = r_B (f - l)$	$R(l) = \frac{R_m}{1-l_p^3} \left[ f l^2 \left( \frac{g+l}{g+f} \right) - l_p^3 \right] (1 + \sigma(C_i^*))^{-1}$

The DEB-tox model has been applied to the nematode *Caenorhabditis elegans* and the waterflea *D. magna* in different contamination situations. In the study by Kooijman and Bedaux (1996), a cadmium exposure induce a mortality during oogenesis (*Hazard model*) whereas an exposure to two chemicals (phenol and 3,4-dichloroanilin) induced indirect effects on reproduction, no identification of one mode of action among the three possible hypotheses (*growth, assimilation and maintenance models*) was possible. A fluoranthene contamination induced a direct effect on reproduction through an increase in costs for egg production (*Cost model*) (Jager and Zimmer, 2012).

The model was previously used to analyse results from toxicological studies with other species. A study on effects of copper in the earthworm *Dendronaena octoedra* showed a reduction in ingestion rate (Jager and Klock, 2010). In *Folsomia candida*, Jager *et al.* (2004) concluded that cadmium induced a decrease in assimilation and triphenyltin induced an increase in maintenance costs. In the same species, two different modes of action were observed during a contamination with the same pollutant, chlorpyrifos. In fact, Jager *et al.* (2007) showed that depending on exposure duration, this toxicant can cause an effect on costs for egg production (after 45 days) or an effect on costs for maintenance (after 120 days). In another study on zebrafish, *Danio rerio*, several modes of action were shown to be involved after an exposure to depleted uranium, depending on the contaminated life stages: an increase in costs for maintenance was shown when the adult stage was exposed; whereas, an increase in mortality during oogenesis and an increase in costs for growth and maturation were demonstrated when early life stages were exposed (Augustine *et al.*, 2012).

#### 2.1.4 The differences between animal and plant DEB models

While DEB-tox models have been used widely in ecotoxicological applications to animals, DEB models for plants are still in the early stages of development. The main difference between an animal model and a plant model is in the uptake of energy. Animals usually eat food which has a very similar (and more or less constant) composition of elements (e.g. C/N ratio) to themselves, which allows for assuming that an animal has one type of generalized reserve. The animal can re-use the assimilated macromolecules such as carbohydrates and proteins with slight modifications to fulfil its need to fuel the various metabolic processes. This generalized reserve density fluctuates in response to food availability, which determines the physiological status of the animal and thus susceptibility to toxicants (Zimmer *et al.*, 2012). The vast literature on DEB applications in animals shows that this assumption, though crude, is reasonable for most applications to animals.

Plants, however, do not "feed" on one food source which has a similar composition to their own: plants use photosynthesis to assimilate inorganic carbon, and additionally assimilate nutrients such as nitrogen, phosphate. From these different sources, the plants have to build up their own macromolecules. In addition photosynthesis itself is not constant as it depends on highly time-variable and weather dependent fluxes of sunlight. Even in the simplest situation of only considering one nutrient and carbon as main components of the macromolecules, co-limitation might need to be considered. Until now, no plant DEB model has been parameterized.

## 2.2 Dependency of radiological stress on dose rate

The DEB-tox model for animals has been developed to analyse data from ecotoxicological tests of chemical compounds (Kooijman and Bedaux, 1996; Jager and Zimmer, 2012). Applying the approach to the case of ionising radiation implies that a metrics is defined for the factor of radiological stress. As described above in the case of chemicals, the metrics for chemical stress is, in most cases, the internalized fraction of the toxic contaminant quantified by  $C_i$  (Figure 3 4), although in some situations, the intensity of effects might as well be correlated to exposure concentration  $C_e$  (Figure 3) when the kinetics are very fast or the stress is caused by the presence of the contaminant at the surface of the organism (Massarin et al., 2011). In other situations, the intensity of effect cannot be related to internal concentration, especially when the body burden is measured and does not follow the same kinetics as observed effects. In order to deal with such situations, Jager *et al.*, (2011) have introduced the concept of damage compartment. Its definition can be found as part of the GUTS model (General Unified Threshold model of Survival) which deals with chronic mortality data. Damage is an abstract concept which incorporates “all kind of biochemical and physiological processes involved in toxicity” and cannot be measured directly. It is an additional toxicodynamic stage which accumulates proportional to the internal concentration and repairs proportional to the actual level (referred to as  $D$ ) in the damage compartment. Similar to internal concentration, the value of  $D$  can be scaled by its bioconcentration factor using the equation:

$$D^* = \frac{k_r}{k_d} D$$

with  $D^*$  the scaled damage level having the units of an internal concentration,  $k_d$  and  $k_r$  the damage accumulation and reparation rates (in  $\text{time}^{-1}$ ), yielding the following simplified equation for the kinetics of the damage:

$$\frac{dD^*}{dt} = k_r (C_i - D^*)$$

if a one-compartment model with first order kinetics is assumed again.

Considering radiological toxicity, level of radiation effects under chronic exposure has been described as a function of dose rate in many studies in the past, as gathered in the FREDERICA database during the EC programs FASSET and ERICA (Williams, 2004; Larsson, 2008). In these studies, effective dose rate resulting in 10 % effect ( $\text{EDR}_{10}$ ) for different endpoints and various species have been derived. These can be regarded as equivalent to  $\text{EC}_{10}$  values for chemical toxicants. Radiological dose (in Gy) measures the amount of energy deposited per mass of exposed tissue, and dose rate is expressed as dose per time. In our studies, we normally deal with small organisms and therefore whole-body exposure, which is why we can use exposure per total body mass over time as a metric for dose rate. Thus, dose rate has the dimension of an internal concentration of radiotoxic stressor (per unit of body volume and time) and can be used in the DEB-tox model as an equivalent of an internal concentration of a chemical toxicant ( $C_i$ ) expressed in mol per body volume and time.

One of the objectives of the present work was to explore the feasibility of applying the DEB-tox in the case of an exposure to ionising radiation using dose rate as an equivalent of internal concentration in the formulation of the stress function.

### ***2.3 Modes of action associated with radiotoxicity: molecular and cellular mechanisms and their consequences for energy budget***

Another major objective of the present work was to identify the metabolic mode of action associated with radiotoxicity. During the STAR program, WP5 task-2 has explored various sub-cellular mechanisms of toxicity for both alpha and gamma radiation. A brief overview of these molecular and cellular mechanisms, as well as those well described in human, makes it possible to suggest most likely DEB-tox modes of action involved during an exposure to ionising radiation (Figure 4).

Biological effects induced by ionising radiation in organisms originate from the deposition of energy from the radioactive material to biomolecules (e.g. DNA, proteins). Ionising radiation can be genotoxic as it interacts with DNA either directly, by deposition of energy in the DNA molecule, or indirectly by formation of free radicals that, via recombination produce reactive oxygen species (ROS) leading to excitations and ionisations. Hence, ionising radiation can lead to DNA lesions, including oxidised and methylated bases, DNA adducts, and single- and double stranded breaks (Steffler, 2004). Production of ROS can additionally be induced through the radiolysis of water. An imbalance between ROS production and ROS scavenging can lead to oxidative stress. This oxidative stress can then indirectly induce DNA damages.

Damage to DNA induces several cellular responses that enable the cell either to eliminate or cope with the damage or to activate a programmed cell death process, presumably to eliminate cells with potentially catastrophic mutations. If DNA damage remains unrepaired or is misrepaired DNA mutations are sustained as single base substitutions, small deletions, recombinations or chromosomal aberrations. Depending on the nature and location of these mutations, this can lead to hereditary effects or stochastic effects.

The DNA damage response reactions include: (a) removal of DNA damage and restoration of the continuity of the DNA duplex; (b) activation of a DNA damage checkpoint, which arrests cell cycle progression so as to allow for repair and prevention of the transmission of damaged or incompletely replicated chromosomes; (c) transcriptional response, which causes changes in the transcription profile that may be beneficial to the cell; and (d) apoptosis, which eliminates heavily damaged or seriously deregulated cells (Sancar et al., 2004). Damage may be either limited to altered DNA bases and abasic sites or extensive like double-strand breaks (DSBs). Nuclear proteins sense this damage and initiate the attachment of protein complexes at the site of the lesion. Subsequently, signal transducers, mediators, and finally, effect or proteins phosphorylate targets (e.g., p53) that eventually results in cell cycle arrest at the G1/S, intra-S, or G2/M checkpoints until the lesion undergoes repair (Houtgraaf et al., 2006). Double strand breaks (DSBs) are a very genotoxic type of DNA damage because several consequences can be induced by the break of both strands of DNA (chromosomal fragmentation, translocations and deletions). The first minutes after induction of DSBs are followed by the extensive phosphorylation of the histone H2AX, followed by DSBs repair mechanisms by homologous recombination (HR) or non-homologous end joining (NHEJ). HR takes place in dividing cells that are in the S or G2 phase, while NHEJ occurs in cells in

G0 or G1 phase. One of the major proteins involved in the NHEJ pathway is the kinase DNA-PK. An overview of the effects induced by low-level chronic gamma radiation in plants and animals has been compiled by Real et al. (2004). More recent studies not included in this review are also available: Gilbin et al. (2008); Vandenhove et al. (2009); Pereira et al. (2011); Simon et al. (2011); Smith et al. (2012); Buisset-Goussen et al. (2014); Parisot et al. (in preparation).

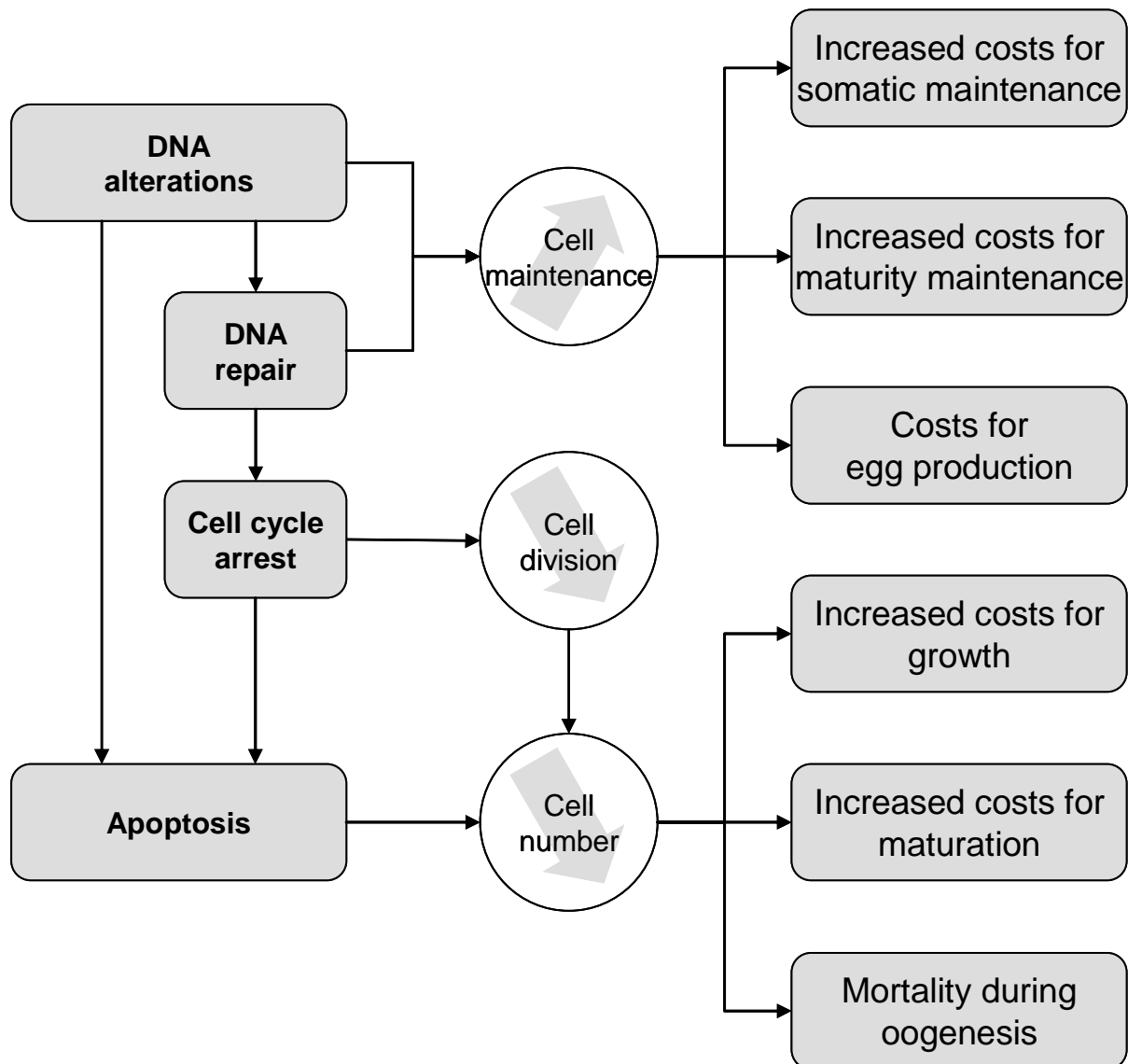


Figure 4: Schematic diagram representing possible consequences of molecular and cellular responses to ionising radiation for the energy budget of organisms. Thereby, it can either be increased costs (e.g. for growth) or a reduction in resource allocation, which will appear as a change in the same model parameter.

A number of studies have published on the impact of chronic gamma irradiation on the invertebrate reproduction parameters in multiple generations (Gilbin et al., 2008; Hertel-Aas et al., 2007; Knowles and Greenwood, 1994, 1997). Similar results are shown in this report including a significant decrease of total number of laid eggs of *C. elegans* exposed to Cs-137 at 500 mGy/h (F0), 42.7 mGy/h (F1) and 8.6 mGy/h(F2). Comparable levels of reprotoxicity were observed between *C. elegans* exposed for 65 h (from eggs stage to young adult stage) and 144 h (from eggs stage to the end of the reproduction process) suggesting that gonads development is particularly sensitive to chronic irradiation. In parallel, we observed that the reduced number of laid eggs was associated to a reduced number of male gametes and to an increase of the relative expression of *egl-1* involved in DNA damage induced germ cell apoptosis. In contrast, no effect on the mitotic cell cycle arrest was observed. These first results support the hypothesis that radiation induced DNA damages mainly underlined the effects observed on reproduction endpoint.

In a recent review of the genotoxic and reprotoxic effects of tritium and external gamma irradiation on aquatic organisms (Adam-Guillermin et al., 2012), the effects of several different dose rates of  $\gamma$  irradiation on aquatic organisms were summarized, and these ranged from 1 mGy/day to 18 Gy/day.

Primary lesions of DNA, such as strand breaks(determined using the Comet assay), were measured in zebra fish cells exposed in vitro(primary cultures) for 24 h to external  $^{137}\text{Cs}$   $\gamma$  rays. An increased sensitivity of male germ cells was seen as compared to hepatocytes (Adam et al. 2006), with a LOEDR for DNA alterations in sperm cells of 1 mGy/day vs. 750 mGy/day for hepatocytes.

A dose-dependent increase of  $\gamma\text{H2AX}$  foci, involved in DNADBS repair, and of micronuclei, was also observed from 10 mGy/day in ZF4 cells (embryonic fibroblasts; Pereira et al.2011). The DSBs NHEJ repair pathway (immunodetection of DNA-PK) was partially inhibited at 100 mGy/day and completely at 750 mGy/day. These increased damages came with a sharp increase of micronuclei, indicative of mitosis death (apoptosis). The same sensitivity was observed in vivo on fertilized eggs exposed to external $\gamma$  irradiation for 1 and 2 days, with an increase of DNA damage observed from a dose of 1 mGy/day (Pereira et al., 2011). Chronic and acute exposures were compared. At low dose and chronic irradiation, more residual DNA damage was induced than at acute irradiation, but embryo development was normal. From 0.3 Gy, a hyper radiosensitivity phenomenon compared to other species was shown for acute exposure with an increase of DNA damage, an impairment of hatching success, and larvae abnormalities. These results suggest a dose-dependent correlation between unrepaired DNA damage and abnormalities in embryo development,

For 2-day-old larvae of the same species (i.e.,5-6 days post-fecundation) that were exposed to external  $^{137}\text{Cs}$   $\gamma$  irradiation at dose rates ranging from 9.6 to 178 mGy/day, genotoxic effects also occurred at doses as low as 29 mGy/day (measured by using the Comet assay; Jarvis and Knowles 2003).For comparable dose rates, no genotoxicity was observed in a marine fish species, the plaice, that were exposed to 6 to 24 mGy/day, for 64 and 167 days (Knowles1999). As suggested by the authors, it is probable that the methods used (micronuclei counts and flow cytometry) may not have been sensitive enough to detect an effect. The chosen life stage (adults) and cell type (erythrocytes) may also have been less sensitive than early life stages and germ cells.

## 2.4 Analysis of relative biological effectiveness: a mechanistic comparison of toxicity between alpha and gamma radiation

Comparing toxic effects between alpha and gamma radiation is a major research goal in STAR WP5. Ionizing radiation can be of different types including energetic particles such as  $^4\text{He}$  nuclei (alpha particle = 2 protons + 2 neutrons), electrons or positrons (beta particles) or energetic photons (gamma rays). In all cases, radiations transfer their energy to the material they move through by direct or indirect ionization. The distance radiation penetrates through a medium depends on its energy and mass. With short wavelengths and a high energy, gamma radiation has a high penetration capacity in different tissues in organisms. With their short penetration range, alpha particles can be attenuated by a paper sheet and cannot penetrate organisms through the outer (dead) cell layer. They become harmful once organisms internalized them.

Radiation effects are assessed through the calculation of the absorbed doses. As each type of radiation interacts differently with matter, the value for absorbed dose in humans is amended by means of a radiation weighting factor ( $w_R$ ) (Table 3). These values are derived by considering the relative biological effectiveness (RBE) of the various radiation types, formulated as the relative amount of ionizing radiation needed to inflict a same amount of damage to an organism (Table 3) and is proportional to the Linear Energy Transfer (LET) of the different radiation types. Values of RBE for humans range from 1 in gamma radiation to 20 in alpha radiation.

Whereas effective dose rate remains relatively constant under external Cs-137 gamma radiation, alpha contamination, as used in our experiments, requires first that Am-241 is internalized in organisms to produce an effective dose rate. Therefore, a proper analysis of RBE first requires that Am-241 biokinetics is quantified, and second properly incorporated into the calculations. Under the circumstance, the DEB-tox approach, which couples a kinetic description of how stress factors build up in organisms with a dynamic description of how toxic stress changes organisms functions over time, appears as the most promising tool. As a case study in this report, the analysis of depleted uranium effects in *D. magna* (section 5.2) illustrates how differing toxicokinetics among generations can strongly alter our understanding of differences in effect severity.

Radiation type	$w_R$
Alpha	20
Beta	1
Protons	2
Photons	1

*Table 3: Radiation weighing factors ( $w_R$ ) for humans (ICRP, 2003). Each value represents the relative biological effectiveness (RBE) of its radiation type, by which absorbed doses can be multiplied to obtain an effective dose.*

## 3 *Caenorhabditis elegans*

### 3.1 Background

This section describes DEB-tox analyses of chronic gamma radiation effects in the nematode *C. elegans* acquired as part of the pilot study conducted at IRSN in collaboration between IRSN and UMB researchers at the end of 2011. The material and methods and results for the experimental part, are described in STAR Deliverable reports 5.1 and 5.3 respectively, with a journal publication in preparation (Lecomte-Pradines *et al.*, in preparation).

A comparative alpha contamination experiment was planned in *C. elegans* in order to acquire the data for an analysis of relative biological effectiveness at the molecular level and at the organism level using DEB-tox. This experiment was cancelled due to the shutdown of IRSN's laboratories for upgrading the air recycling system, making it impossible to safely handle the alpha emitter, Am-241, in their facilities.

### 3.2 Formulation of a DEB-tox model applied to chronic external gamma radiation

#### 3.2.1 Model assumptions

##### 3.2.1.1 Stress factors

The model aims to test whether an energy-based model can help understanding effects of chronic external gamma radiation in *C. elegans*. Several hypotheses were tested concerning the factor of stress related to radiation exposure:

- In the first hypothesis (Figure 5), stress intensity was assumed to be correlated to dose rate  $DR$  as explained in section 2.2, so that effect intensity was immediately at its maximum value. We formulated the equation for the stress function  $\sigma$ , with dose rate  $DR$  (in  $\text{mGy h}^{-1}$ ) appearing where the internal concentration  $C_i^*$  was used for chemicals:

$$\begin{cases} \sigma(DR) = 0 & \text{if } DR < NEDR \\ \sigma(DR) = b \cdot (DR - NEDR) & \text{if } DR \geq NEDR \end{cases}$$

with radiological stress affecting the energy budget when the dose rate  $DR$  exceeds a threshold value named the no-effect dose rate  $NEDR$  with  $b$  (in  $\text{mGy}^{-1} \text{h}$ ) the slope of the stress intensity (Figure 6).

- If the time course of stress does not follow the kinetics of dose rate, we can consider a second hypothesis (Figure 5), that the intensity of effect is correlated to a level of damage  $D$ . This damage is accumulated proportionally to dose rate  $DR$  and repairs proportionally to the actual level in the damage compartment (Jager *et al.*, 2011). Analogous to the scaling of the internal concentration  $C_i^*$ , the value of  $D$  can be scaled by a factor similar to the bioconcentration factor using the equation:

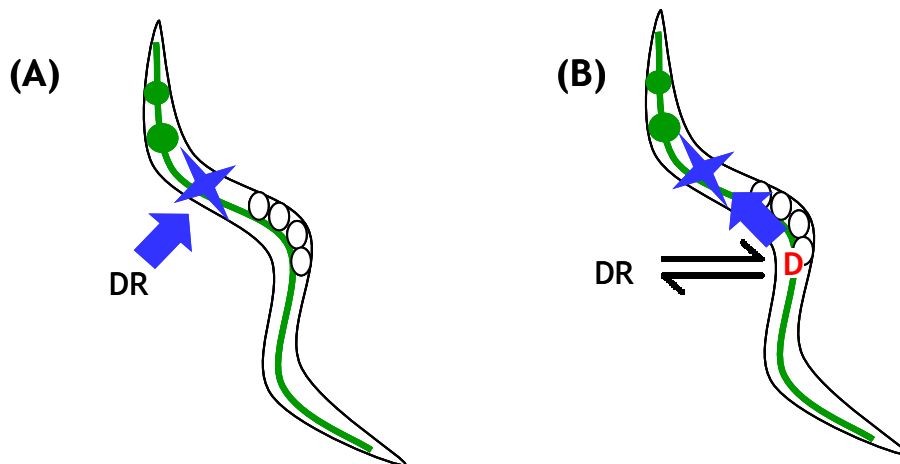


Figure 5: Schematic diagram of *C. elegans* with the eggs (white circles), food items (green circles) passing through the columns (green line) and the actual observed effect (blue star), representing different hypotheses for the kinetics of the radiological stress: (A) with immediate induction of effect on energy budget (with stress correlated to exposure dose rate DR); (B) with slower kinetics of effect on energy budget (correlated to a damage level D).

$$D^* = \frac{k_r}{k_d} D$$

with  $D^*$  the scaled damage level having units of dose rate ( $\text{mGy h}^{-1}$ ),  $k_d$  and  $k_r$  the damage accumulation and reparation rates (in  $\text{time}^{-1}$ ), yielding the following simplified equation for the kinetics of the damage (Figure 6) if a one-compartment model with first order kinetics is assumed:

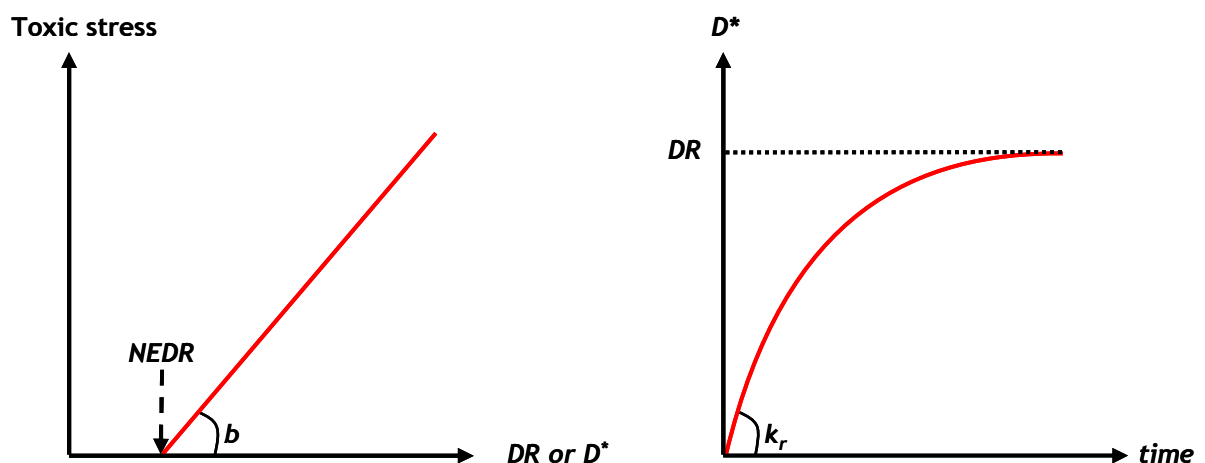


Figure 6: Stress intensity as a function of dose rate DR or scaled damage  $D^*$  (with NEDR, the no-effect dose rate) and changes in scaled damage  $D^*$  over time.

$$\frac{dD^*}{dt} = k_r (DR - D^*)$$

Under this assumption, the stress function  $\sigma$  takes the following form, with intensity correlated to scaled damage  $D^*$  (in  $\text{mGy h}^{-1}$ ):

$$\begin{cases} \sigma(D^*) = 0 & \text{if } D^* < NEDR \\ \sigma(D^*) = b \cdot (D^* - NEDR) & \text{if } D^* \geq NEDR \end{cases}$$

with radiological stress affecting the energy budget when the scaled damage  $D^*$  exceeds a threshold value named the no-effect dose rate  $NEDR$  with  $b$  (in  $\text{mGy}^{-1} \text{ h}$ ) the slope of the stress intensity.

### 3.2.1.2 Growth and reproduction differential equations depending on mode of action

Experimental results (STAR deliverable report 5.3) indicated strong effects on reproduction and a possible effect on growth. Reduction in size at the highest tested dose rate was very slight with a significant reduction in Von Bertalanffy growth rate pointing to a possible increase in costs for growth and maturation. Other modes of action cannot be firmly ruled out due to the great variability among individuals. As a consequence, five different hypotheses can be considered in order to identify the mode of action associated to chronic external gamma radiation.

Differential equations are given in Table 4 depending on the considered mode of action, with  $\sigma$  radiological stress correlated to dose rate  $DR$  or damage level  $D^*$ . Equations show an additional stress  $S_f$  affecting energy intake  $f$ . This stress is assumed in order to take account of the sigmoid growth curve observed in nematodes (Byerly *et al.*, 1976) reflecting a slower growth in early stages than in old ones. Knight *et al.* (2002) explains this slow initial growth as a result of a possible size-dependent food imitation, small individuals having small mouth cavities. Under this assumption, the stress  $S_f$  on ingestion is formulated as a function of size (Jager *et al.*, 2005), as follows:

$$S_f(l) = 1 - \left( 1 + \frac{l_f^3}{l^3} \right)^{-1}$$

with  $l$  the scaled body length and  $l_f$  the scaled body length at which ingestion rate is half of maximum.

Another particularity of the DEB model in nematode considers the limitation of lifetime reproduction to a maximum  $R_{max}$  due to a limited number of male gametes. This maximum is dealt with by Jager *et al.* (2005) using a threshold condition on reproduction rate  $R(l)$ :

$$R(l) = 0 \text{ if } R \geq R_{max}$$

with  $R$  the cumulated reproduction.

Table 4: Sets of differential equations for growth and reproduction based on a simplified DEB-tox model (assuming constant exposure conditions) with radiological stress  $\sigma$  causing one of the five modes of action (as a function of dose rate DR or damage level  $D^*$ ) and a morphological stress  $S_f$  affecting ingestion in nematodes (as a function of body length).

Tested mode of action	Growth	Reproduction
	$l(0) = l_b$	$R(l) = 0 \text{ if } l < l_p$
Costs for growth and maturation	$\frac{dl}{dt} = r_B \frac{f+g}{f(1-S_f)+g(1+\sigma)} (f(1-S_f)-l)$	$R(l) = \frac{R_m}{1-l_p^3} \left[ f(1-S_f)l^2 \left( \frac{g(1+\sigma)+l}{g(1+\sigma)+f(1-S_f)} \right) - l_p^3 \right]$
Costs for somatic and maturity maintenance	$\frac{dl}{dt} = r_B \frac{f+g}{f(1-S_f)+g} (f(1-S_f)-l(1+\sigma))$	$R(l) = \frac{R_m}{1-l_p^3} (1+\sigma) \left[ f(1-S_f)l^2 \left( \frac{g(1+\sigma)^{-1}+l}{g+f(1-S_f)} \right) - l_p^3 \right]$
Reduction in assimilation	$\frac{dl}{dt} = r_B \frac{f+g}{f(1-S_f)(1-\sigma)+g} (f(1-S_f)(1-\sigma)-l)$	$R(l) = \frac{R_m}{1-l_p^3} \left[ f(1-S_f)(1-\sigma)l^2 \left( \frac{g+l}{g+f(1-S_f)(1-\sigma)} \right) - l_p^3 \right]$
Mortality during oogenesis	$\frac{dl}{dt} = r_B \frac{f+g}{f(1-S_f)+g} (f(1-S_f)-l)$	$R(l) = \frac{R_m}{1-l_p^3} \left[ f(1-S_f)l^2 \left( \frac{g+l}{g+f(1-S_f)} \right) - l_p^3 \right] e^{-\sigma}$
Costs for production of eggs	$\frac{dl}{dt} = r_B \frac{f+g}{f(1-S_f)+g} (f(1-S_f)-l)$	$R(l) = \frac{R_m}{1-l_p^3} \left[ f(1-S_f)l^2 \left( \frac{g+l}{g+f(1-S_f)} \right) - l_p^3 \right] (1+\sigma)^{-1}$

Male gametogenesis might be directly affected by toxicity and this is taken into account through maximum cumulated reproduction  $R_{max}$  using the following equation:

$$R_{max} = \frac{R_{max}(0)}{(1 + k_2 \cdot \sigma)}$$

where  $R_{max}(0)$  is the maximum reproduction in the unexposed control and  $k_2$  measures the stress on  $R_{max}$  relative to stress  $\sigma$  on the energy budget.

Goussen *et al.* (in press) suggests a modification in the nematode DEB model in order to allow small nematodes to access a fraction  $1 - \alpha$  of food whatever their length and grow when food is partially limiting. This modification makes the model applicable to a wider range of food conditions. For parsimony, we choose not to use this modification, to avoid the cost of the additional parameter ( $\alpha$ ) considering that the pilot study was conducted in *ad libitum* food conditions. A second modification is also suggested to take account of the gradual shutoff of egg laying when the cumulated reproduction  $R$  gets close to maximum  $R_{max}$ . This gradual shutoff is obtained by Goussen *et al.* (in press) adding a term of the form:

$$\frac{R_{max} - R}{R_{max}}$$

so that:  $R(l) \rightarrow 0$  when  $R \rightarrow R_{max}$ , with no cost in term of number of parameters. In our present work, we test how this modification (hereafter referred to as “Gradual”) fits the chronic gamma radiation effect dataset compared to the standard DEB-tox with the threshold condition on  $R$  (hereafter referred to as “Threshold”)

### 3.2.1.3 Exposure conditions

The model is used to analyze experimental data from the experimental study described in STAR Deliverable reports 5.1 (Material and methods) and 5.3 (Results). The tested range of gamma dose rates ( $^{137}\text{Cs}$  solid and liquid sources) includes 0, 0.042, 0.318, 3.38, 21.3 and 26.8 mGy h<sup>-1</sup>. Each nematode is exposed and followed individually. Nematodes survival is monitored daily for 26 days, while their growth and reproduction is monitored for 11 days. Number of replicates per dose rate ranges from 27 nematodes at 26.8 mGy h<sup>-1</sup> to 30 nematodes at other dose rates.

## 3.2.2 Parameterization

### 3.2.2.1 Method for fitting growth and reproduction curves

In agreement with Jager *et al.* (2004), parameterization is performed simultaneously for growth and reproduction using the least squares criterion. Simultaneous fitting is necessary to take account of the close relationship between both endpoints.

DEB-tox equations are parameterized separately between:

- “physiological” parameters (namely  $l_b$ ,  $l_f$  and  $l_p$  the scaled body length at birth, at 50% the maximum ingestion rate and at puberty  $L_m$ ,  $r_B$  the Von Bertalanffy growth rate,  $R_m$  the maximum reproduction rate and  $R_{max}$  the maximum cumulated reproduction) which

describe how unexposed organisms behave physiologically based on the control unexposed dataset;

- “toxicokinetic / toxicodynamic” parameters (namely *NEDR* the no-effect dose rate, *b* the slope of stress intensity, *k<sub>r</sub>* the damage reparation rate and *k<sub>2</sub>* the stress ratio between energy budget and maximum cumulated reproduction) which describe how the control model is modified as a function of dose rate based on the “exposed” dataset once the physiological parameters are estimated.

Every combination of hypotheses regarding the nature of the stress factor applied (*DR* or *D\**), the nature of the mode of action (growth, assimilation, maintenance, cost or hazard model) and the model used to deal with the maximum cumulated reproduction *R<sub>max</sub>* (threshold condition or gradual shutoff) was tested during calculations.

### 3.2.2.2 Least squares criterion

The parameterization is achieved by minimizing a weighted sum of squares *SSQ(tot)*. To do so, a mean sum of squares *SSQ(Y)* is calculated for each endpoint *Y* (growth and reproduction) using the following equation:

$$SSQ(Y) = \sum_j \frac{1}{n_r(Y, j)} \sum_r^{n_r(Y, j)} \left( \frac{\hat{Y}_{ji} - Y_{jir}}{\sigma(Y_{ji})} \right)^2$$

with *n<sub>r</sub>(Y, j)* the replicate number of observations of *Y* in condition *j* (including all time points *i*), *Ŷ<sub>ji</sub>* the estimated value of *Y* in condition *j* at time *i*, *Y<sub>jir</sub>* a replicate observation of *Y* in condition *j* at time *i* and, *σ(Y<sub>ij</sub>)* the standard deviation of *Y<sub>jir</sub>* observations in condition *j* at time *i*. Contributions of growth and reproduction to the minimized criterion are balanced using *SSQ<sub>min</sub>(Y)* as a weighting factor for each value of *SSQ(Y)*:

$$SSQ(tot) = \sum_Y \frac{SSQ(Y)}{SSQ_{min}(Y)}$$

where *SSQ<sub>min</sub>(Y)* is a minimum sum of squares, used to correct the relative importance of reproduction in the criterion, calculated according to the following equation:

$$SSQ_{min}(Y) = \sum_j \frac{1}{n_r(Y, j)} \sum_r^{n_r(Y, j)} \left( \frac{\bar{Y}_{ji} - Y_{jir}}{\sigma(Y_{ji})} \right)^2$$

with *Ȳ<sub>ji</sub>* the mean value of *Y* in condition *j* at time *i*.

### 3.2.2.3 Confidence intervals and model selection

Confidence intervals for the different parameters and model outputs are built using a bootstrap technique. A bootstrap resampling classically deals with independent observations, whereas our dataset is composed of individual series, each describing changes in size and reproduction over time in a same nematode. As a consequence, our data include a certain degree of correlation among time points and between endpoints. In order to take account of this correlation, datasets are simulated by randomly resampling from each dose rate the same number of individuals as the observed dataset (with replacement, e.g. possibility to select the

same individual several times). Once an individual is drawn, its whole growth curve and reproduction curve are included in the sampled dataset. On each sampled dataset, models are adjusted to determine parameters as described previously. This procedure is performed 5,000 times.

Because the different hypotheses involve different numbers of parameters among modes of action and among stress factors, model selection is achieved using Akaike Information Criteria (*AIC*) defined as:

$$AIC = -2\ln(L) + 2d$$

where  $d$  is the number of parameters in the model, and  $\ln(L)$  is the log-likelihood of the model. Here, *AIC* is calculated for each hypothesis as:

$$AIC = \sum_Y SSQ(Y) + \frac{2d}{N}$$

where  $N$  is the total number of observations. *AIC* are calculated for every bootstrap dataset and the frequency of each model yielding the lowest *AIC* (*i.e.* the best hypothesis considering the number of parameters) is calculated.

### 3.2.3 Results

#### 3.2.3.1 Estimated “physiological” parameters

All the results presented here will be published in Lecomte-Pradines *et al.* (in preparation). Estimated “physiological” parameters for growth and reproduction of unexposed nematodes in control conditions are presented in Table 5. All parameter values are in good agreement with the literature (Jager *et al.*, 2005; Swain *et al.*, 2010). One can see that the two options for the reproduction model yield approximately similar values, with the exception of maximum reproduction rate  $R_m$  which is significantly lower in the “threshold condition” model than in

Table 5: “Physiological” DEB parameters estimated for the two reproduction models based on data from control nematodes with 95% confidence intervals into brackets (obtained based on 5000 bootstrap datasets).

Symbol	Unit	Definition	Reproduction model	
			Threshold	Gradual
$g$	-	Energy investment ratio	10.7 [6.09 – 2.38]	9.34 [2.53 – 17.4]
$L_b$	-	Scaled length at birth	0.194 [0.185 – 0.205]	0.194 [0.185 – 0.205]
$l_f$	-	Scaled length at which ingestion is 50% of maximum	0.262 [0.251 – 0.284]	0.271 [0.250 – 0.283]
$L_m$	μm	Maximum length	1290 [1250 – 1335]	1290 [1250 – 1335]
$r_B$	d <sup>-1</sup>	von Bertalanffy growth rate	0.753 [0.703 – 1.12]	0.830 [0.680 – 0.914]
$l_p$	-	Scaled length at puberty	0.677 [0.668 – 0.776]	0.725 [0.690 – 0.748]
$R_m$	egg d <sup>-1</sup>	Maximum reproduction rate	203 [189 – 287]	333 [301 – 447]
$R_{max}$	egg	Maximum cumulated reproduction	260 [248 – 272]	260 [248 – 272]

the “Gradual shutoff” model. This is due to the fact that reproductive rate when cumulated reproduction gets close to  $R_{max}$  is underestimated by more than 50% when the gradual shutoff is not taken into account.

### 3.2.3.2 Comparison of fits among hypotheses

Table 6 reports values of  $SSQ$  obtained for the various tested combinations of hypotheses. For each combination (e.g. a stress factor  $DR$  or  $D^*$  × a nature for the mode of action × an option for the reproduction model), values of the least weighted sum of squares  $SSQ(tot)$  and of its un-weighted components for growth and reproduction, respectively  $SSQ(gro)$  and

Table 6: Least weighted sums of squares  $SSQ(tot)$ , their un-weighted components for growth and reproduction, respectively  $SSQ(gro)$  and  $SSQ(repro)$ , the associated  $AIC$  and the percent frequency of models yielding the lowest  $AIC$ , obtained for the different combinations of hypotheses based on data from exposed nematodes.

Stress factor		$DR$			
Hypotheses	$SSQ(gro)$	$SSQ(repro)$	$SSQ(tot)$	$AIC$	%
<b>Threshold</b>					
Growth	6.88 [6.75 – 12.6]	5.59 [5.34 – 12.7]	2.73 [2.78 – 5.15]	14.63	14.9
Assimilation	7.08 [6.92 – 13.0]	5.59 [5.17 – 12.9]	2.77 [2.77 – 5.29]	14.83	7.5
Maintenance	7.20 [6.97 – 12.9]	5.59 [5.19 – 12.9]	2.80 [2.80– 5.35]	14.95	6.4
Cost	7.45 [7.24 – 15.3]	5.75 [5.27 – 13.2]	2.89 [2.90– 5.74]	15.37	1.5
Hazard	7.45 [7.24 – 15.3]	5.75 [5.27 – 13.2]	2.89 [2.90– 5.74]	15.36	6.4
<b>Gradual</b>					
Growth	7.06 [6.68– 11.4]	5.76 [5.42– 9.66]	2.81 [2.79– 4.44]	14.97	30.7
Assimilation	7.25 [6.85– 11.7]	6.22 [5.38– 9.79]	2.96 [2.81 – 4.54]	15.62	3.4
Maintenance	7.39 [6.91 – 11.9]	5.78 [5.25– 9.92]	2.88 [2.81 – 4.61]	15.32	4.1
Cost	7.84 [7.16– 14.3]	5.80 [5.39 – 9.95]	2.98 [2.89 – 5.11]	15.79	1.1
Hazard	7.84 [7.16– 14.3]	5.79 [5.39 – 10.0]	2.98 [2.89 – 5.11]	15.79	1.2
Stress factor		$D^*$			
Hypotheses	$SSQ(gro)$	$SSQ(repro)$	$SSQ(tot)$	$AIC$	%
<b>Threshold</b>					
Growth	6.88 [6.75 – 12.6]	5.59 [5.34 – 12.7]	2.73 [2.78 – 5.15]	14.63	0.0
Assimilation	7.08 [6.92 – 13.0]	5.59 [5.17 – 12.9]	2.77 [2.77 – 5.29]	14.83	<0.1
Maintenance	7.20 [6.97 – 12.9]	5.59 [5.19 – 12.9]	2.80 [2.80– 5.35]	14.95	0.0
Cost	7.45 [7.24 – 15.3]	5.75 [5.27 – 13.2]	2.89 [2.90– 5.74]	15.37	<0.1
Hazard	7.45 [7.24 – 15.3]	5.75 [5.27 – 13.2]	2.89 [2.90– 5.74]	15.36	<0.1
<b>Gradual</b>					
Growth	7.20 [6.74 – 12.4]	5.73 [5.41 – 9.39]	2.83 [2.82 – 4.60]	15.08	14.0
Assimilation	7.08 [7.17– 13.0]	6.03 [5.40– 9.81]	2.88 [2.89 – 4.83]	15.27	1.6
Maintenance	7.36 [7.24 – 13.2]	7.28 [5.50 – 9.71]	3.22 [2.95 – 4.84]	16.79	4.3
Cost	7.84 [7.16– 14.3]	5.89 [5.42– 9.25]	3.00 [2.89 – 5.07]	15.88	0.8
Hazard	7.84 [7.16– 14.3]	5.87 [5.41– 9.24]	3.00 [2.89 – 5.04]	15.86	2.0

$SSQ(repro)$ , are provided.  $SSQ(gro)$  and  $SSQ(repro)$  represent the average distance between measured size and reproduction and their corresponding model predictions, small values of  $SSQ(gro)$  and  $SSQ(repro)$  indicating that the parameterized model describes well the observed datasets. The AIC estimates the ability of the model to describe the data, taking account of the number of fitted parameters (best models requiring the smallest number of parameters).

The comparison shows that whatever the considered hypotheses on stress factor and on the reproduction model, growth is always worst described (highest values for  $SSQ(gro)$ ) when a direct effect on reproduction (“cost” or “hazard” models) is assumed. This observation confirms that growth is affected, even slightly, when nematodes are exposed to chronic gamma radiation. The model yields the highest frequency of best fits (representing altogether  $\approx 60\%$  of lowest AIC) when an increase in costs for growth and maturation (“Growth” model) is assumed as the mode of action, independent of the stress factor, dose rate  $DR$  or damage  $D^*$  and the reproduction model, “Threshold” or “Gradual” (in grey in Table 6). However, the damage compartment  $D^*$  can never fit as well as dose rate  $DR$ , because it involves an additional parameter  $k_r$  (frequency of lowest AIC  $\approx 0\%$  and  $14\%$  respectively when the “Threshold” and the “Gradual” reproduction models are considered). Between the two best options, both times obtained with an increase in costs for growth and maturation (“Growth” model) with dose rate  $DR$  as the stress factor, a narrower confidence interval is obtained for  $SSQ(tot)$  with the “Gradual” reproduction model ([2.79 – 4.44]) than with the “Threshold” model ([2.78 - 5.15]). As a consequence, despite a higher  $SSQ(tot)$  calculated on the observed dataset, the “Gradual” reproduction model yields the higher frequency of lowest AIC ( $>30\%$ ) than the “Threshold” reproduction model ( $\approx 15\%$ ).

### 3.2.3.3 Estimated “toxicokinetic and toxicodynamic” parameters

Values of “toxicokinetic and toxicodynamic” parameters obtained for the four best fits, giving the lowest least weighted sums of squares  $SSQ(tot)$  and/or the highest frequency of lowest AIC, are presented in Table 7.

The value of  $NEDR$  ranges from  $\approx 2$  to  $\approx 900$  mGy h<sup>-1</sup>. A very wide associated uncertainty is observed, especially when dose rate is considered as the stress factor (with confidence interval covering up to 7 orders of magnitude). This uncertainty in the model is significantly reduced when toxic stress is assumed to depend on a damage  $D^*$ . In fact, introducing  $D^*$  narrows confidence intervals on  $NEDR$  to two orders of magnitude when the “Threshold” reproduction model is considered and down to one order of magnitude when the “Gradual” reproduction model is considered. Thus, improving the description of the reproduction in the control nematodes strongly contributes to reducing the uncertainty in the toxicokinetic/toxicodynamic model, although some of the uncertainty is transferred to the damage repair rate.

The value of  $k_2$ , the stress on  $R_{max}$  relative to the stress on energy budget, ranges from 0.5 to 2.3 (with confidence intervals covering  $\approx 1$  order of magnitude) depending on the tested hypothesis. This indicates that the increase in costs for growth is not sufficient to explain the observed reduction in the total number of eggs produced per nematode and that a direct effect on reproduction must be considered, whatever the stress factor and the model of reproduction.

Table 7: “Toxicokinetic and toxicodynamic” DEB-tox parameters yielding the best fits (i.e. giving the lowest least weighted sums of squares  $SSQ(tot)$  and/or the highest frequency of lowest AIC), obtained assuming an increase in costs for growth and maturation correlated to dose rate  $DR$  or a damage  $D^*$  and using the “Threshold” or “Gradual” reproduction models, based on data from exposed nematodes with 95% confidence intervals into brackets (obtained based on 5000 bootstrap datasets).

Symbol	Unit	Definition	Reproduction model	
			Threshold	Gradual
<b>Stress factor: dose rate <math>DR</math></b>				
$NEDR$	$mGy\ h^{-1}$	No-effect dose rate	604 [ $<0.001 - 19000$ ]	2.53 [ $<0.001 - 8810$ ]
$b$	$mGy^{-1}\ h$	Slope of stress intensity	$2.87 [1.27 - 6.89] \times 10^{-6}$	$3.28 [1.41 - 5.04] \times 10^{-6}$
$k_2$	-	Stress on $R_{max}$ relative to stress on energy budget	2.30 [1.05 - 6.00]	1.52 [0.667–5.00]
<b>Stress factor :damage <math>D^*</math></b>				
$NEDR$	$mGy\ h^{-1}$	No-effect dose rate	899 [687 - 21700]	810 [490 - 1140]
$b$	$mGy^{-1}\ h$	Slope of stress intensity	$1.30 [0.05-2.00] \times 10^{-3}$	$1.07 [0.50 - 9.05] \times 10^{-5}$
$k_r$	$d^{-1}$	Damage reparation rate	0.005 [0.001–1.32]	0.378 [0.004–0.524]
$k_2$	-	Stress on $R_{max}$ relative to stress on energy budget	1.11 [0.939 – 23.3]	0.509 [0.324 - 1.06]

### 3.2.3.4 Growth, reproduction and stress factors curves

The ability of the model to describe the observed data assuming different hypotheses is illustrated in Figures 7 A to C. Graphically, growth and reproduction data are well described for all cases (independent of the stress factor or the model of reproduction), with the exception of reproduction around days 4 to 6 where the gradual reductive rate is not correctly taken in to account by the “Threshold” model at the dose rate of  $3.38\ mGy\ h^{-1}$  (Figure 7A). In comparison, the “Gradual” shutoff near  $R_{max}$  offers a better description of actual observations (Figures 7 B and C).

With the “Gradual” model of reproduction and radiological stress correlated to a cumulated damage (Figures 7C), the level of damage exhibits a strong uncertainty. This uncertainty is particularly visible with increasing dose rate and implies that a fraction of the (bootstrap) simulated nematodes remains below the  $NEDR$  (estimated between  $0.49$  and  $1.14\ mGy\ h^{-1}$ ) while the scaled damage ranges from 1 to and unaffected even at the highest dose rates. This uncertainty is also present under other hypotheses and results from the no-effect dose rate when the model assumes that radiological stress is correlated to dose rate  $NEDR$ . In other words, the model tells either that 1) severity of radiological stress is correlated to an accurately estimated factor (dose rate) but we do not accurately know at which dose rate nematodes energy budget is affected or 2) that we accurately know at which level of factor (damage) nematodes energy budget is affected but we cannot accurately estimate this factor in nematodes.

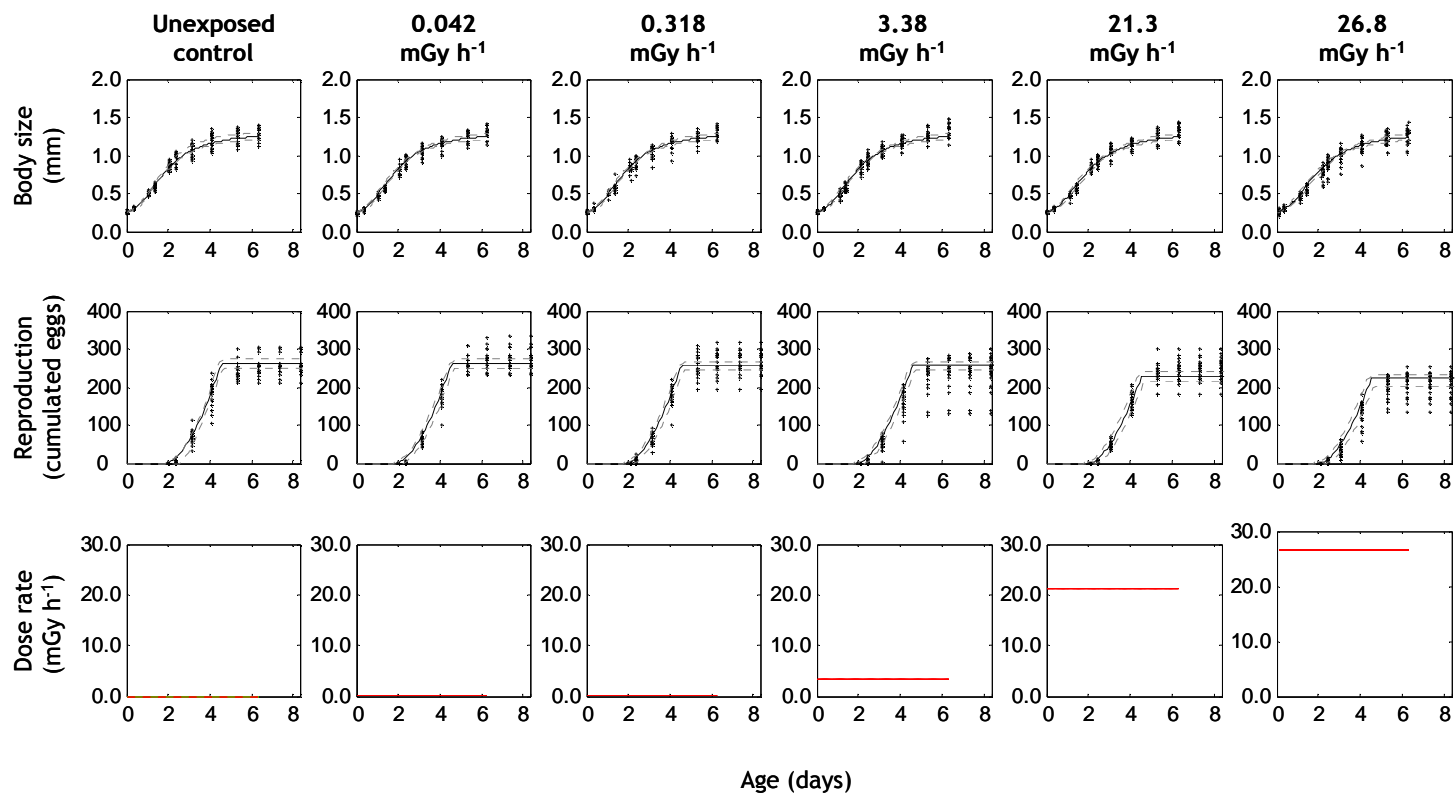


Figure 7A: Fitted growth and reproduction curves to data, with a “Threshold” model of reproduction, with an indirect increase in costs for growth and maturation and a direct increase in costs for reproduction (as the modes of action of gamma radiation) correlated to exposure dose rate DR (in red). ‘+’ observed data; Continuous line: model predictions; Dotted lines: model 95%-confidence intervals.

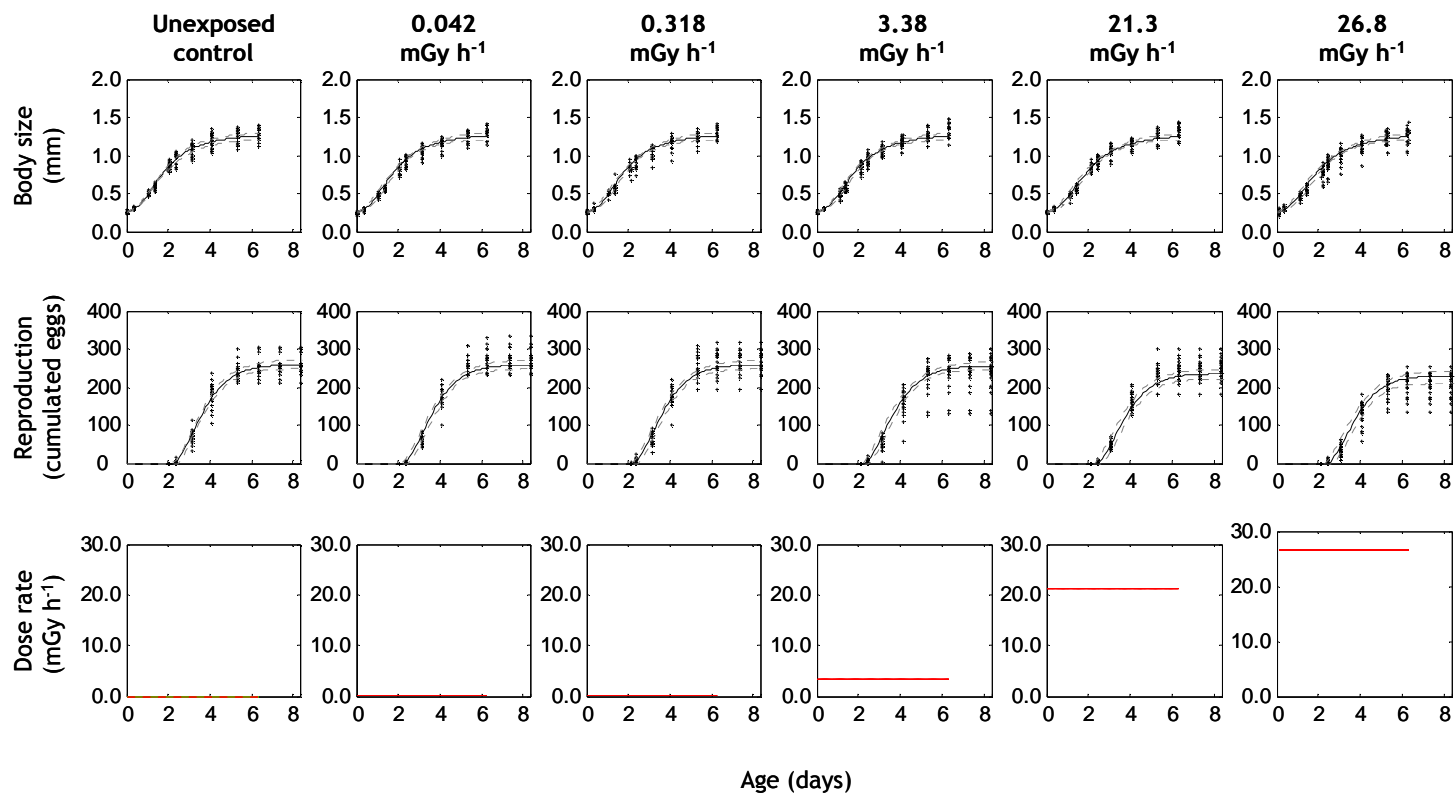


Figure 7B: Fitted growth and reproduction curves to data, with a “Gradual” model of reproduction, with an indirect increase in costs for growth and maturation and a direct increase in costs for reproduction (as the modes of action of gamma radiation) correlated to exposure dose rate DR (in red). ‘+’ observed data; Continuous line: model predictions; Dotted lines: model 95%-confidence intervals.

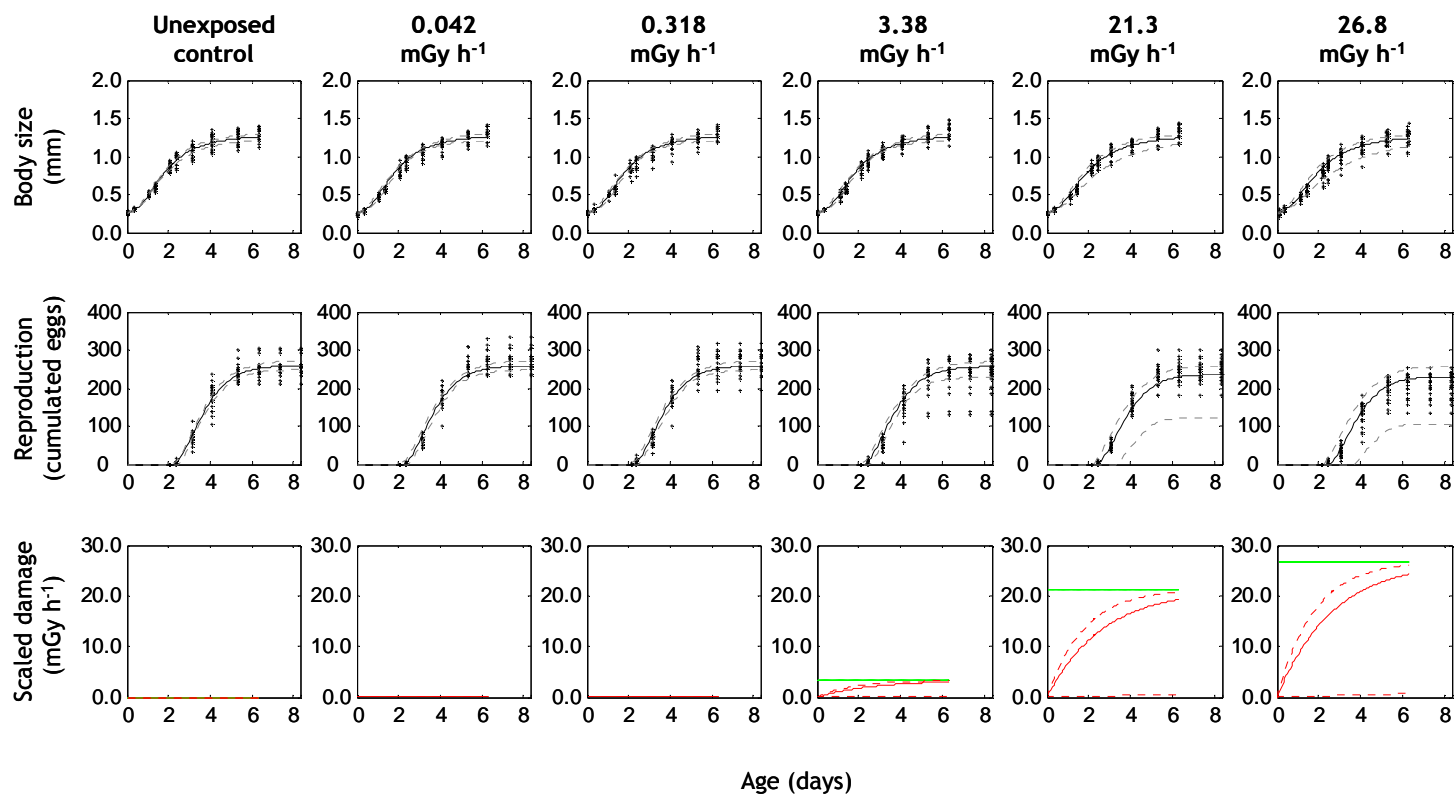


Figure 7C: Fitted growth and reproduction curves to data with a “Gradual” model of reproduction, with an indirect increase in costs for growth and maturation and a direct increase in costs for reproduction (as the modes of action of gamma radiation) correlated to a cumulated damage (in red). ‘+’ observed data; Continuous line: model predictions; Dotted lines: model 95%-confidence intervals. Green dashed lines represent exposure dose rates DR.

## 4 *Daphnia magna*

### 4.1 Introduction

This section describes the approach used by IRSN to link effect severity to (DNA) inheritable damage during a multigenerational exposure. The approach was developed to explain the increase in effect severity during exposure to depleted uranium for 3 generations. The conclusion that, beside a direct effect on assimilation associated to histological damage on the digestive epithelium, depleted uranium has an effect on costs for growth and maturation that can be correlated to the accumulation, transmission and elimination of inheritable damage. The same approach is now ready to be applied to the case of alpha and gamma radiation in a multigeneration context.

### 4.2 *DEB-tox applied to a multigenerational depleted uranium exposure*

#### 4.2.1 Background

The study of Massarin *et al.* (2010) demonstrated that exposure to depleted uranium primarily affects carbon assimilation in daphnids and caused effects on survival, growth and reproduction which increased in severity over successively exposed generations. DEB-tox analyses (Massarin *et al.*, 2011) underlined that observed effects on growth and reproduction can be explained by a decrease in assimilation correlated to external concentration. This interpretation is in good agreement with the observation of histological damage on the digestive epithelium by photon microscopy. The second conclusion of the study was that the observed increase in effect severity across generations can be described with different stress functions which are specific of each generation (Figure 8). A decrease in no-effect concentration *NEC* and an increase in slope of effect intensity *b* was considered from one generation to the next, resulting in an increasing toxic stress across generations at a given concentration.

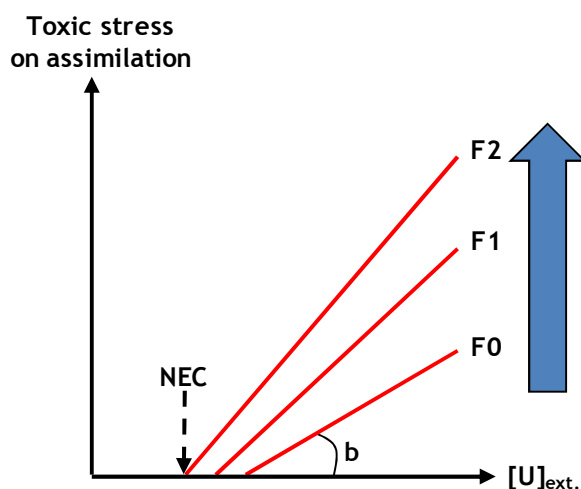


Figure 8: Stress intensity as a function of generation and external uranium concentration  $[U]_{ext}$  obtained by Massarin *et al.* (2011) after analysing results from Massarin *et al.* (2010).

This increase in severity of effects on survival, growth and reproduction across generations remains unexplained because the mechanism underlying changes in toxic stress on assimilation is not understood. The increasing sensitivity to U-depl does necessarily originate from a variable which can be transmitted from one generation to the next. This variable is not internalized uranium concentration because a similar value is measured in every concentration (Massarin *et al.*, 2010). A combination of two toxic stresses – one linked to the exposure concentration and a second to an inheritable damage level (Jager *et al.*, 2011) – is thus foreseen. The two stress factors might act together on assimilation or involve a second mode of action independent of the decrease in assimilation.

Plaire *et al.* (2013) tested the hypothesis that the increase in effect severity is caused by the accumulation and transmission of DNA alterations during a multigenerational exposure to depleted uranium. DNA alterations were measured using the RAPD-qPCR technique (randomly amplified polymorphic DNA by quantitative polymerase chain reaction), leading to the conclusion that in two exposure regimes (continuous exposure during every life stages, post-hatching exposure during juvenile and adult stages) an accumulation and transmission of DNA alterations occurred across generations, together with an increase in effect severity on survival, growth and reproduction. Furthermore, in a third exposure regime where daphnids were exposed only during the embryonic stage, transient DNA alterations observed during the first generation become non-significant in the second and third generations, while no increase in effect severity was observed. Effects on growth and reproduction remained visible after daphnids were returned to a clean medium upon hatching, but no significant difference was reported across generations.

#### 4.2.2 Formulation of a dual-stress DEB-tox model

##### 4.2.2.1 *Model assumptions*

The model aims to test whether an inheritable damage causing a second source of stress acting through a second mode of action can help explain the transgenerational changes in effect severity. We introduce a model with two stress factors: one being internal or exposure uranium concentration ( $C_i^*$  or  $C_e$ ) inducing a decrease in assimilation, as described by Massarin *et al.* (2011), and the other being a damage level ( $D$ ) necessarily inheritable from one generation to the next, in order to explain the observed increase in effect intensity. The two stress factors are assumed to act independently through two stress functions  $\sigma_1$  and  $\sigma_2$  represented by the equations below.

Several hypotheses are tested concerning the factor of stress applied to assimilation, in agreement with Massarin *et al.* (2011):

- In a first hypothesis, decrease in assimilation is correlated to exposure concentration (Figure 9), such that effect intensity is immediately at its maximum, in agreement with depleted uranium in the gut tract inducing an effect on assimilation directly at the surface of the digestive epithelium:

$$\begin{cases} \sigma_1(C_e) = 0 & \text{if } C_e < NEC_1 \\ \sigma_1(C_e) = b_1 \cdot (C_e - NEC_1) & \text{if } C_e \geq NEC_1 \end{cases}$$

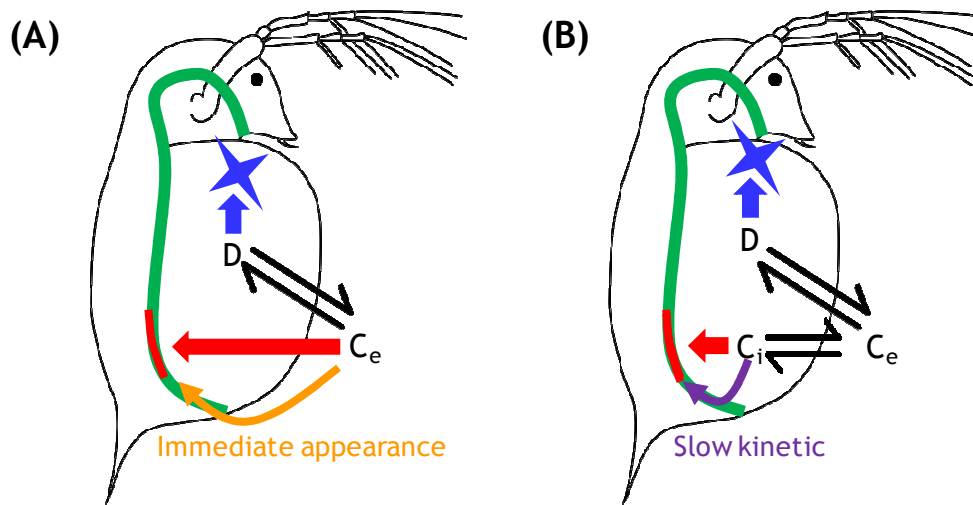


Figure 9: Schematic diagram of a *Daphnia* representing different hypotheses for the kinetics of the dual-stress model: (A) with immediate induction of effect on assimilation (with stress correlated to exposure concentration  $C_e$ ); (B) with slower kinetics of effect on assimilation (correlated to internal concentration  $C_i$ );  $D$ : damage level inducing the second mode of action. For symbols, see Figure 5.

with  $C_e$  the exposure concentration,  $NEC_I$  the no-effect-on-assimilation concentration and  $b_I$  the slope of effect intensity on assimilation.

- In a second hypothesis, decrease in assimilation is correlated to internal concentration ruled by the standard DEB-tox kinetics (Figure 9):

$$\frac{dC_i^*}{dt} = C_e \frac{k_e}{l} - C_i^* \left( \frac{k_e}{l} + \frac{d}{dt} \ln l^3 \right)$$

supporting the idea that depleted uranium needs to accumulate in intestine epithelial cells and might be influenced by dilution during growth of the animal before it causes the effect on assimilation:

$$\begin{cases} \sigma_I(C_i^*) = 0 & \text{if } C_i^* < NEC_I \\ \sigma_I(C_i^*) = b \cdot (C_i^* - NEC_I) & \text{if } C_i^* \geq NEC_I \end{cases}$$

with  $C_i^*$  the scaled internal concentration,  $NEC_I$  the no-effect-on-assimilation concentration and  $b_I$  the slope of effect intensity on assimilation.

As the uranium concentration ( $C_i^*$ ) is scaled by its bioconcentration factor, the damage level ( $D^*$ ) taking the dimension of a uranium concentration (Jager *et al.*, 2011) is scaled as follows:

$$D^* = \frac{k_r}{k_d} D$$

with  $k_d$  and  $k_r$  the damage accumulation and reparation rates. The kinetics of the damage compartment is described by a simple one-compartment model with first-order equation (Jager *et al.*, 2011):

$$\frac{dD^*}{dt} = k_r(C_e - D^*)$$

Although accumulation in the damage compartment is most likely to be correlated to internal concentration (because depleted uranium needs to be internalized in cells before it can induce DNA alterations), we prefer to keep damage accumulation proportional to external concentration (Figure 9) and avoid the strong correlation between elimination rate  $k_e$  and reparation rate  $k_r$  which would make the evaluation of these two parameters statistically more difficult.

$$\begin{cases} \sigma_2(D^*) = 0 & \text{if } D^* < NEC_2 \\ \sigma_2(D^*) = b_2 \cdot (D^* - NEC_2) & \text{if } D^* \geq NEC_2 \end{cases}$$

with  $D^*$  the scaled damage level associated to the second mode of action,  $NEC_2$  the no-effect damage level and  $b_2$  the slope of effect intensity.

As formulated, the model has many implications for the interpretation of the links between exposure level and molecular responses and between molecular responses and their consequences for the organism: First, the model does not attempt to estimate the concentration at which molecular responses start to be induced, because it assumes that the slightest concentration induces a molecular response; Second, the model assumes that the slightest molecular response does not necessarily cause a toxic stress and explores the molecular response (i.e. the damage level) at which a toxic stress is induced on the organism's energy budget.

#### 4.2.2.2 Hypotheses on mode(s) of action

Five different hypotheses can be considered in order to identify a second mode of action associated to the damage compartment (Table 8). One has to note that both effects on reproduction and effects on growth increase in severity across generations. This observation rules out direct modes of action on reproduction (Cost and Hazard models) as the possible

Table 8: Combination of tested modes of action

Mode of action 1	Mode of action 2	Symbols	Tested
Assimilation	Growth	A-G	yes
	Assimilation	A-A	yes
	Maintenance	A-M	yes
	Cost	A-C	no
	Hazard	A-H	no

second mode of action, considering that the second mode of action must explain the increase in effect severity on growth. For this reason, we will only consider assimilation combined with one of the three indirect models in the calculations (A-G, A-A, and A-M).

#### 4.2.2.3 Growth and reproduction differential equations

Sets of differential equations used to achieve adjustments are presented in Table 9. In these equations, stress  $\sigma_1$  corresponding to the decrease in assimilation and stress  $\sigma_2$  corresponding to the increase in effect severity are combined according to the nature of the second mode of action. In previous applications of DEB-tox to *D. magna*, the energy investment ratio  $g$  has been set equal to 1 (Billoir *et al.*, 2008; Massarin *et al.*, 2011). On the other hand, daphnids in experiments are fed *ad libitum* in experiments (Massarin *et al.*, 2010; Plaire *et al.*, 2013) so scaled nutritional response  $f$  is fixed to 1.

#### 4.2.2.4 Exposure regimes

The model is used to analyze experimental data from Massarin *et al.* (2010) and Plaire *et al.* (2013). Different exposure regimes must be considered to cover all the tested situations (Table 10). In Plaire *et al.* (2013), the same life stages were exposed between generations F0 and F1 (experiments 1, 2 and 3). The tested range of exposure concentrations includes 0; 2; 9,9; 22,2 and 50  $\mu\text{g L}^{-1}$ . In Massarin *et al.* (2010), different life stages were exposed among generations F0, F1 and F2 (experiments 4, 5 and 6). The tested range of exposure concentrations included 0; 10; 25 and 75  $\mu\text{g L}^{-1}$ .

Table 9: Sets of differential equations for growth and reproduction based on a simplified DEB-tox model (assuming constant exposure conditions) with two stresses  $\sigma_1$  (causing a decrease in assimilation as a function of uranium concentration) and  $\sigma_2$  (causing one of the five modes of action as a function of damage level).

Combination of modes of action	Growth	Reproduction
	$l(0) = l_b$	$R(l) = 0$ if $l < l_p$
A-G	$\frac{dl}{dt} = r_B \frac{f+g}{f(1-\sigma_1)+g(1+\sigma_2)} (f(1-\sigma_1)-l)$	$R(l) = \frac{R_m}{1-l_p^3} \left[ f(1-\sigma_1) l^2 \left( \frac{g(1+\sigma_2)+l}{g(1+\sigma_2)+f(1-\sigma_1)} \right) - l_p^3 \right]$
A-M	$\frac{dl}{dt} = r_B \frac{f+g}{f(1-\sigma_1)+g} (f(1-\sigma_1)-l(1+\sigma_2))$	$R(l) = \frac{R_m}{1-l_p^3} (1+\sigma_2) \left[ f(1-\sigma_1) l^2 \left( \frac{g(1+\sigma_2)^{-1}+l}{g+f(1-\sigma_1)} \right) - l_p^3 \right]$
A-A	$\frac{dl}{dt} = r_B \frac{f+g}{f(1-\sigma_1)(1-\sigma_2)+g} (f(1-\sigma_1)(1-\sigma_2)-l)$	$R(l) = \frac{R_m}{1-l_p^3} \left[ f(1-\sigma_1)(1-\sigma_2) l^2 \left( \frac{g+l}{g+f(1-\sigma_1)(1-\sigma_2)} \right) - l_p^3 \right]$
A-H	$\frac{dl}{dt} = r_B \frac{f+g}{f(1-\sigma_1)+g} (f(1-\sigma_1)-l)$	$R(l) = \frac{R_m}{1-l_p^3} \left[ f(1-\sigma_1) l^2 \left( \frac{g+l}{g+f(1-\sigma_1)} \right) - l_p^3 \right] e^{-\sigma_2}$
A-C	$\frac{dl}{dt} = r_B \frac{f+g}{f(1-\sigma_1)+g} (f(1-\sigma_1)-l)$	$R(l) = \frac{R_m}{1-l_p^3} \left[ f(1-\sigma_1) l^2 \left( \frac{g+l}{g+f(1-\sigma_1)} \right) - l_p^3 \right] (1+\sigma_2)^{-1}$

Table 10: Summary of exposure regimes (grey cells after end of experiment)

Experiment	F0 exposure		F1 exposure		F2 exposure	
	Embryo	Post-hatching	Embryo	Post-hatching	Embryo	Post-hatching
1	YES	YES	YES	YES		
2	YES	NO	YES	NO		
3	NO	YES	NO	YES		
4	NO	YES	YES	YES	YES	YES
5	NO	YES	YES	NO		
6	NO	YES	YES	YES	YES	NO

#### 4.2.2.5 Hypotheses on inheritability and reversibility

With exposure concentrations varying among life stages and generations in experiments 2, 3, 5 and 6 (Massarin *et al.*, 2010 and Plaire *et al.*, 2013), it is necessary to draw hypotheses on how toxic stress may change over time when exposed daphnids are returned to a clean medium or from exposed females to their offspring.

Inheritability, which describes how the damage level is transmitted from daphnids to their eggs, is a necessary condition in order to explain the increase in effect severity from one generation to the next. This is simply achieved by setting the initial damage level in eggs at the value cumulated in mothers upon brood deposition (Figure 10A). However, toxic stress affecting assimilation is caused by alterations of daphnids digestive epithelium and is, by its nature, most unlikely to be transmitted to offspring. Initial stress level in eggs is therefore set back to zero independent of the value cumulated in mothers upon brood deposition (Figure 10B).

Experimental results from Massarin *et al.* (2010) and Plaire *et al.* (2013) showed that exposure during the embryonic stage and/or during previous generations can induce significant effects, even after daphnids are returned to a clean medium. This observation implies that the kinetics of recovery might be slow or partially irreversible. This can be achieved by low uranium elimination rate  $k_e$  and/or damage reparation rate  $k_r$  (Figure 11A). In order to allow a fast kinetics of toxic stress on assimilation as described by Massarin *et al.* (2011), we also considered the hypothesis of complete irreversibility, where decrease in stress on assimilation and/or the second mode of action is, more drastically, no longer possible (Figure 11B).

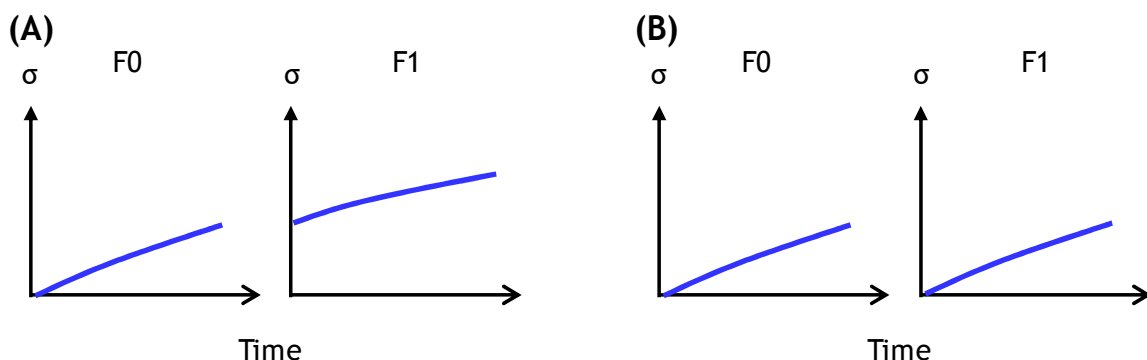


Figure 10: Schematic diagram representing the different hypotheses for the inheritability of toxic stress during a continuous exposure: (A) with transmission of stress from mothers F0 to offspring F1; (B) with no transmission of stress from mothers F0 to offspring F1.

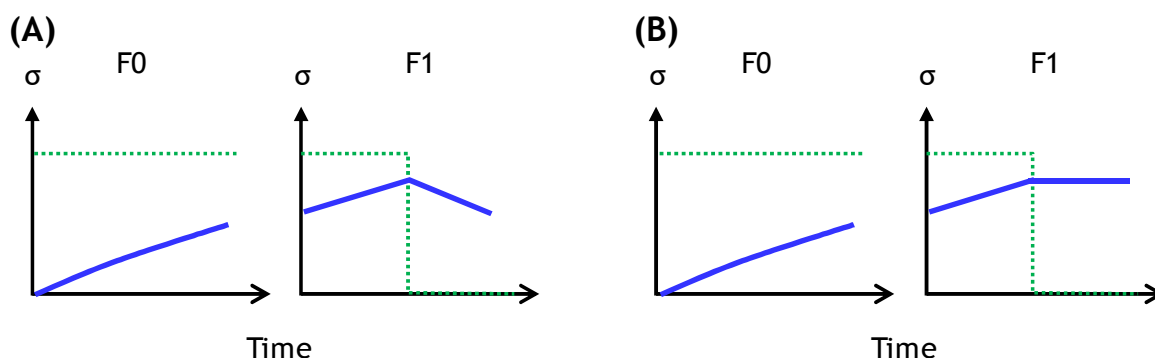


Figure 11: Schematic diagram representing the different hypotheses for reversibility of toxic stress after a return in uncontaminated medium in generation F1: (A) with reversibility of toxic stress; (B) with no reversibility of toxic stress. Green dotted lines represent exposure concentration.

#### 4.2.3 Parameterization

##### 4.2.3.1 *Method for fitting growth and reproduction curves*

As explained for nematodes, parameterization is performed simultaneously for growth and reproduction in agreement with Jager *et al.* (2004) using the least squares criterion (see section 3.2.2.1).

Reproduction data is expressed as cumulated egg mass, results from Massarin *et al.* (2010) and Plaire *et al.* (2013) having shown that mass per egg is correlated to daphnid size. Larger females producing eggs of heavier mass, using egg mass as a metric of energy investment in reproduction seems judicious to accurately quantify effects on both growth and reproduction (Massarin *et al.*, 2011).

#### 4.2.4 Results

##### 4.2.4.1 Estimated “physiological” parameters

Estimated “physiological” parameters for growth and reproduction of unexposed daphnids in control conditions are presented for each experiment and generation in Table 11. Results confirm the previous conclusion by Massarin *et al.* (2011) that control growth and reproduction differ slightly among generations in experiments 4, 5 and 6. The situation also occurs in experiment 1 by Plaire *et al.* (2013). In every case, obtained results remain valid with respect to the criterion in the OECD guidelines of 60 neonates produced over 21 days. The difference might be due to fluctuating experimental conditions such as food quality which is difficult to maintain. Their influence is taken into account by considering specific parameterizations for the differing generations.

##### 4.2.4.2 Comparison of fits among hypotheses

Table 12 reports values of  $SSQ$  obtained for the various tested combinations of hypotheses, and the fits on cumulated egg mass are shown in Figure 12. For each combination (*e.g.* a stress factor for assimilation  $\times$  a nature for the second mode of action  $\times$  a hypothesis on the reversibility of stresses), values of the least weighted sum of squares  $SSQ(tot)$  and of its un-weighted components for growth and reproduction, respectively  $SSQ(gro)$  and  $SSQ(repro)$ , are provided.  $SSQ(gro)$  and  $SSQ(repro)$  represent the average distance between measured size and reproduction and their corresponding model predictions, small values of  $SSQ(gro)$  and  $SSQ(repro)$  indicating that the parameterized model describes well the observed datasets.

Table 11: “Physiological” DEB-tox parameters estimated for each experiment and generation based on control datasets from Massarin *et al.* (2010) for experiments 1 to 3 and Plaire *et al.* (2013) for experiments 4 to 6.

Experiments and generations		Parameters				
		$L_b$ (mm)	$L_p$ (mm)	$L_m$ (mm)	$r_B$ ( $j^{-1}$ )	$R_m$ ( $\mu g.oeufs.j^{-1}$ )
Exp 1	F0	0.958	0.639	4.137	0.145	82.126
	F1	1.014	0.535	4.290	0.155	91.511
Exp 2	F0	1.002	0.622	3.871	0.209	45.502
	F1	1.030				
Exp 3	F0	1.002	0.622	3.871	0.209	45.502
	F1	1.030				
Exp 4	F0	1.002	0.570	4.353	0.145	77.197
	F1	1.078	0.656	4.246	0.135	75.685
	F2	1.024	0.520	4.346	0.127	100.403
Exp 5	F0	1.002	0.570	4.353	0.145	77.197
	F1'	1.076	0.656	4.245	0.135	75.652
Exp 6	F0	1.002	0.570	4.353	0.145	77.197
	F1	1.078	0.656	4.246	0.135	75.685
	F2'	1.024	0.521	4.346	0.127	100.403

Table 12: Least weighted sums of squares  $SSQ(tot)$  and their un-weighted components for growth and reproduction, respectively  $SSQ(gro)$  and  $SSQ(repro)$ , obtained for the different combinations of hypotheses based on data from exposed daphnids from Massarin *et al.* (2010) and Plaire *et al.* (2013).

Hypothesis	Stress factor Assimilation					
	$C_e$			$C_i^*$		
	$SSQ(gro)$	$SSQ(repro)$	$SSQ(tot)$	$SSQ(gro)$	$SSQ(repro)$	$SSQ(tot)$
<b>Reversible stress on assimilation and damage</b>						
A-G	27640	5976	0.5628	27640	5976	0.5630
A-A	27649	6786	0.5649	27649	6786	0.5652
A-M	27673	7129	0.5661	27653	6737	0.5646
<b>Reversible stress on assimilation and irreversible damage</b>						
A-G	27636	5988	0.5628	27647	5531	0.5620
A-A	27651	6800	0.5649	27649	6788	0.5649
A-M	27675	7015	0.5660	27675	6621	0.5650
<b>Irreversible stress on assimilation and reversible damage</b>						
A-G	27640	5976	0.5628	27621	5455	0.5613
A-A	27649	6786	0.5649	27637	6042	0.5630
A-M	27673	7129	0.5661	27675	6251	0.5655
<b>Irreversible stress on assimilation and damage</b>						
A-G	27636	5988	0.5628	27623	5804	0.5621
A-A	27651	6800	0.5649	27655	6146	0.5634
A-M	27675	7015	0.5660	27675	6836	0.5655

The comparison shows that relative variations in  $SSQ$  are much greater for reproduction than for growth, i.e. that the model describes daphnid growth relatively well, independent of the tested hypothesis. Whatever the considered hypotheses on stress factor for assimilation and on the reversibility of stresses, the model always describes the data best when an increase in costs for growth and maturation, as a second mode of action, is assumed. This observation is true for both growth and reproduction. Furthermore, the model yields better fits when internal concentration  $C_i^*$ , rather than exposure concentration  $C_e$ , is taken as the stress factor for assimilation (grey values in Table 12). Finally, among the different hypotheses on reversibility, the overall best fit is simultaneously obtained for growth and reproduction when stress on assimilation is irreversible and damage is reversible, in good agreement with the observation by Plaire *et al.* (2013) that DNA alterations can be repaired when daphnids are returned to an uncontaminated medium. Under the second best hypothesis (reversible stress on assimilation and irreversible damage), the model underestimates observed effects on reproduction in generation F0 after an embryonic exposure and a return to uncontaminated medium (Figure 12).

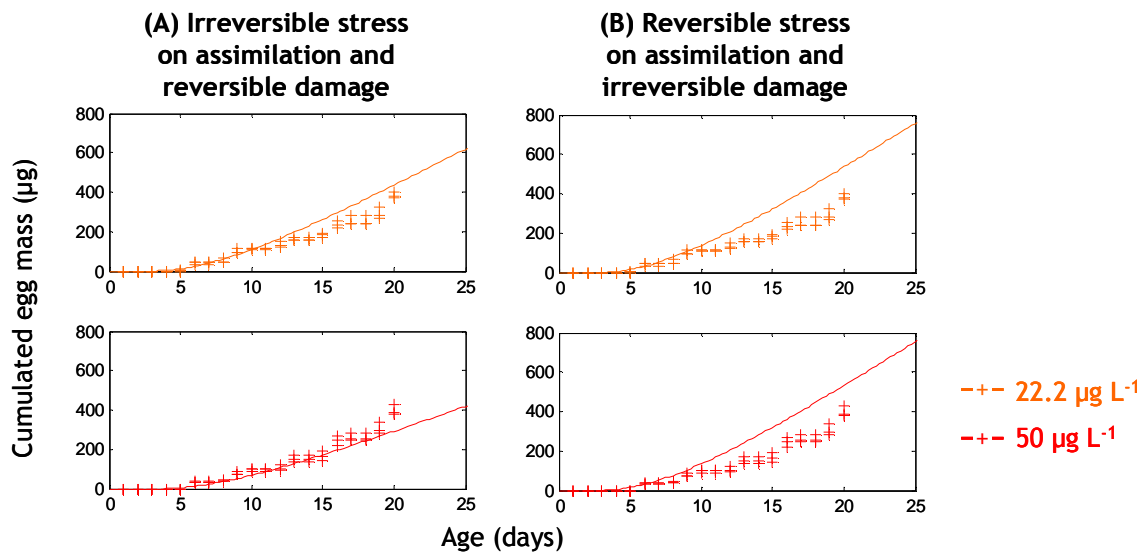


Figure 12: Fitted reproduction curves depending on hypothesis of reversibility. Fits to data from experiment 2 generation F0 (exposure during the embryonic stage) by Plaire *et al.* (2013), with effect on assimilation correlated to internal concentration  $C_i^*$  and costs for growth and maturation (as a second mode of action) correlated to an inheritable damage  $D^*$ . ‘+’ observed data; Continuous line: model predictions.

#### 4.2.4.3 Growth and reproduction curves

The ability of the model to describe observed data in different exposure scenarios is illustrated in Figures 13 and 14. Graphically, growth and reproduction data are well described for all situations (independent of the experiment, generation and concentration), except 1) at the concentration of  $75 \mu\text{g L}^{-1}$  in generation F1 (Figures 14A) where effect on growth is underestimated, and 2) at the concentration of  $25 \mu\text{g L}^{-1}$  in generation F2 (Figures 14A) where effect on reproduction is strongly underestimated. Both cases represent extreme situations (highest tested concentrations in generations F1 and F2) with possible strong mortality (Massarin *et al.*, 2010).

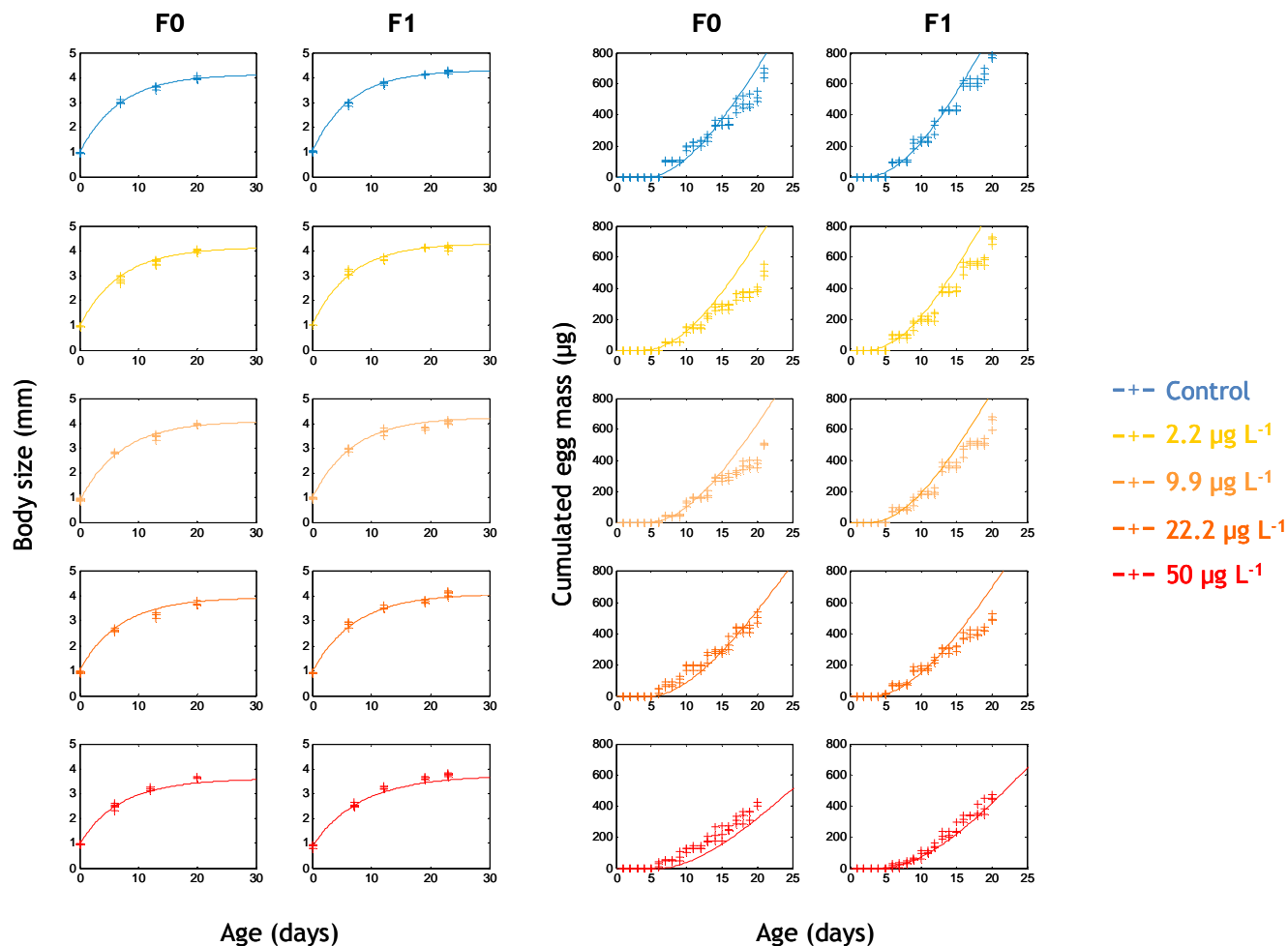


Figure 13A: Fitted growth and reproduction curves to data in experiment 1 (continuous exposure) from Plaire et al. (2013), with an irreversible reduction in assimilation correlated to internal concentration  $C_i^*$  and a reversible increase in costs for growth and maturation (as a second mode of action) correlated to an inheritable damage  $D^*$ . '+' observed data; Continuous line: model predictions.

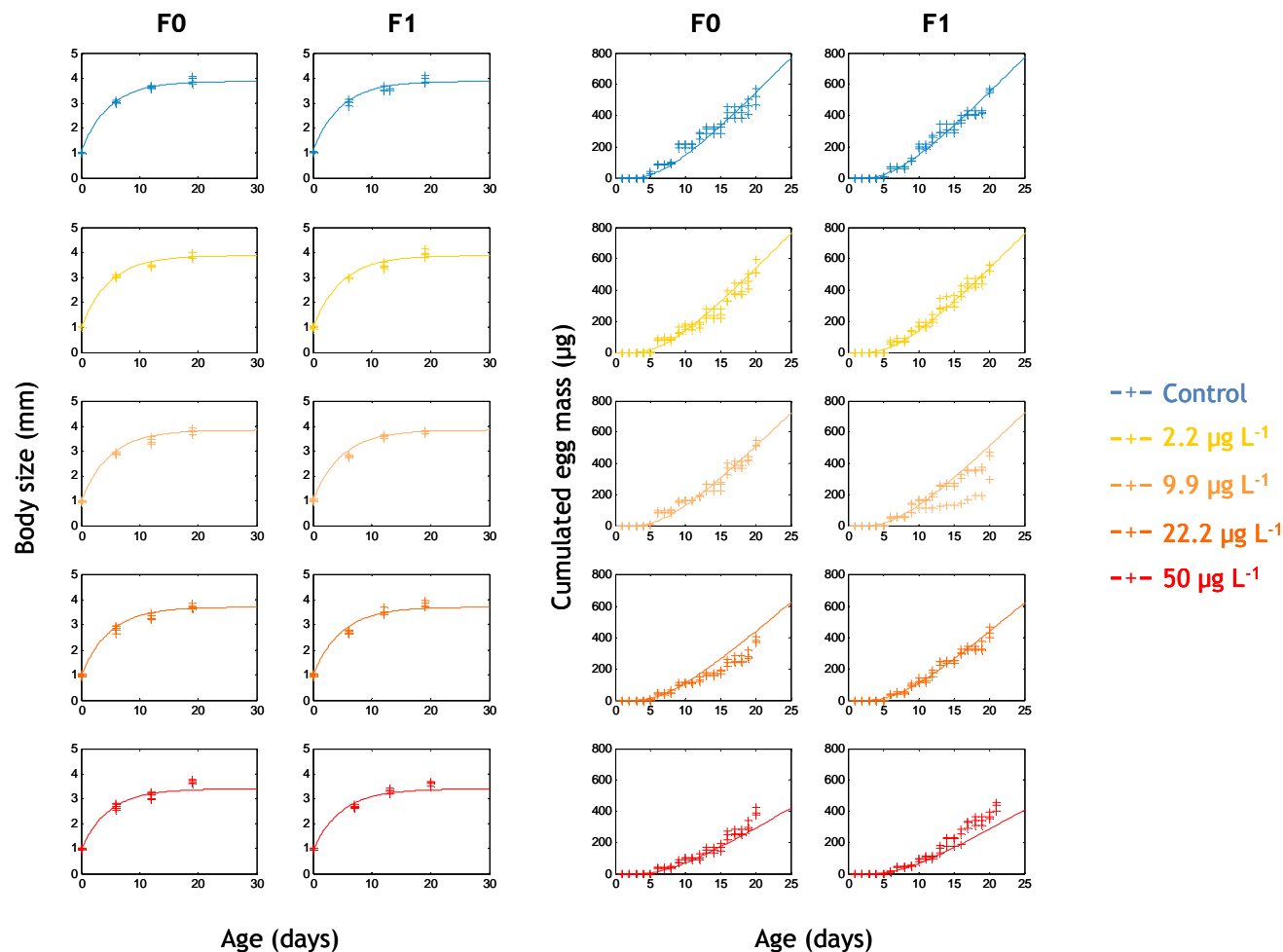


Figure 13B: Fitted growth and reproduction curves to data in experiment 2 (exposure during the embryonic stage) from Plaire et al. (2013), with an irreversible reduction in assimilation correlated to internal concentration  $C_i^*$  and a reversible increase in costs for growth and maturation (as a second mode of action) correlated to an inheritable damage  $D^*$ . ‘+’ observed data; Continuous line: model predictions.

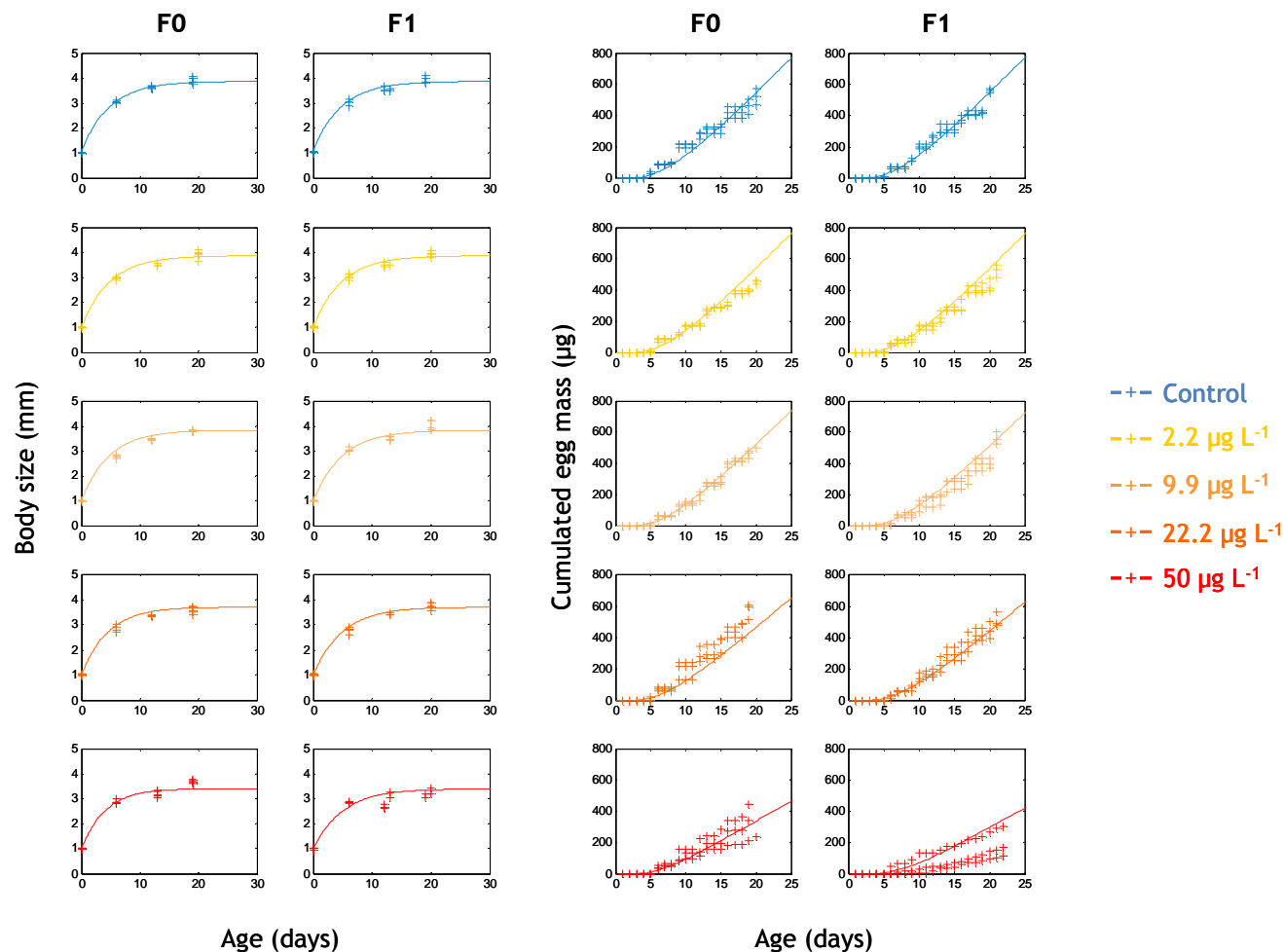


Figure 13C: Fitted growth and reproduction curves to data in experiment 3 (exposure after hatching) from Plaire et al. (2013), with an irreversible reduction in assimilation correlated to internal concentration  $C_i^*$  and a reversible increase in costs for growth and maturation (as a second mode of action) correlated to an inheritable damage  $D^*$ . ‘+’ observed data; Continuous line: model predictions.

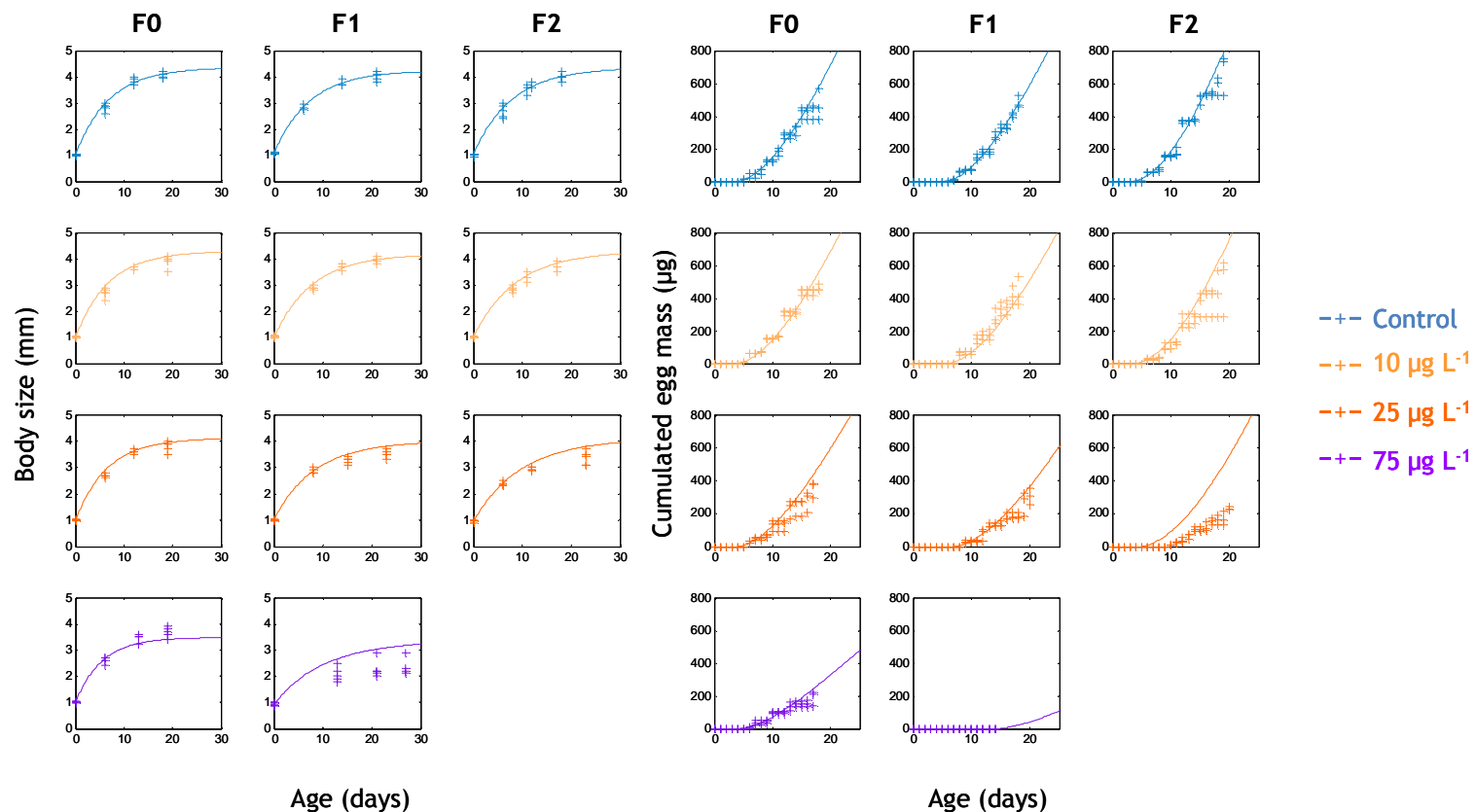


Figure 14A: Fitted growth and reproduction curves to data in experiment 4 (continuous exposure) from Massarin et al. (2010), with an irreversible reduction in assimilation correlated to internal concentration  $C_i^*$  and a reversible increase in costs for growth and maturation (as a second mode of action) correlated to an inheritable damage  $D^*$ . ‘+’ observed data; Line: model predictions.

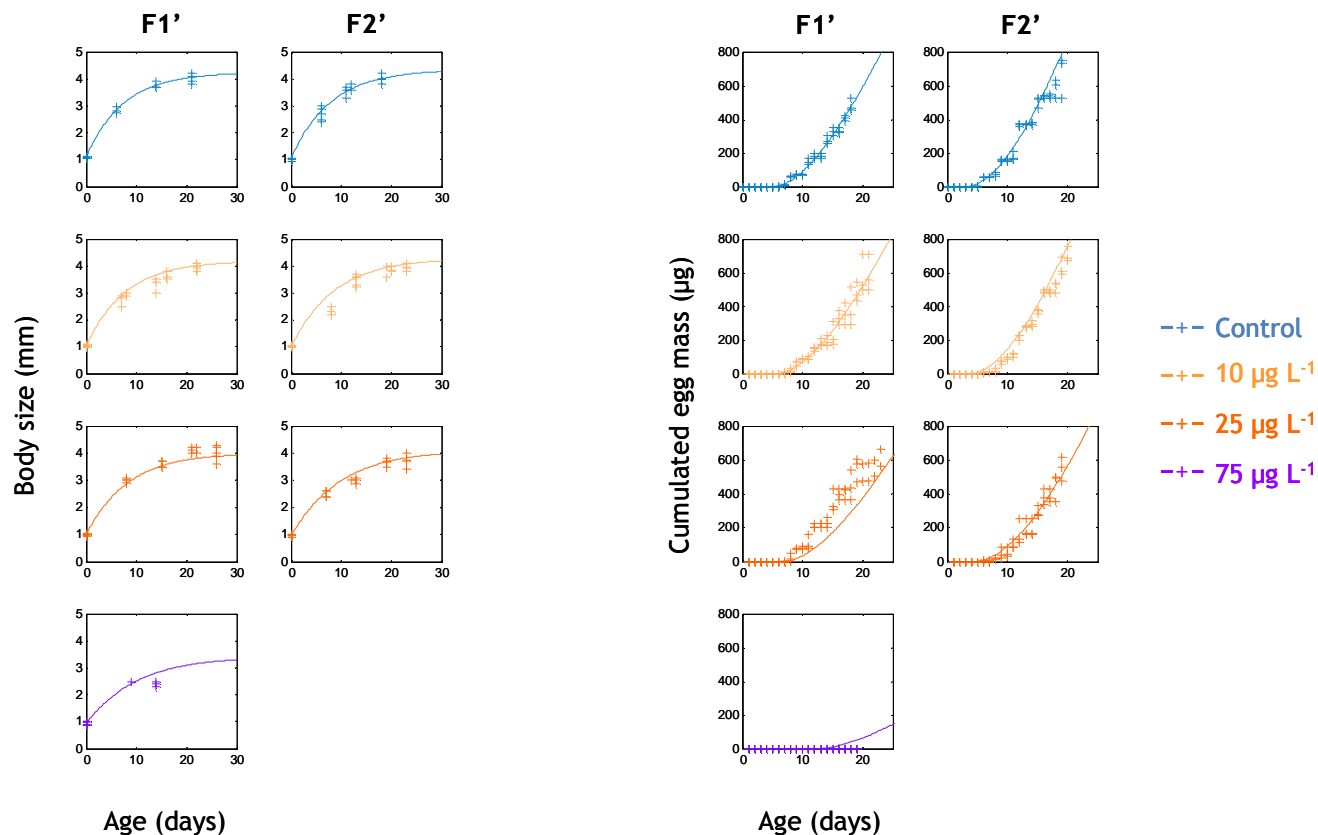


Figure 14B: Fitted growth and reproduction curves to data in experiments 5 and 6 (recovery in generation F1' or F2') from Massarin et al. (2010), with an irreversible reduction in assimilation correlated to internal concentration  $C_i^*$  and a reversible increase in costs for growth and maturation (as a second mode of action) correlated to an inheritable damage  $D^*$ . '+' observed data; Line: model predictions.

#### 4.2.4.4 Stress factors curves

Predicted curves for the stress factors, internal concentration  $C_i^*$  (causing an irreversible reduction in assimilation) and inheritable damage  $D^*$  (causing a reversible increase in costs for growth and maturation) are presented in Figure 15. These curves clarify the contribution of each stress factor to the observed increase in effect severity across generations:

- When daphnids are exposed during the embryonic stage, like in experiments 1 and 2 generations F0 and F1 (Figure 15A) and in experiments 4, 5 and 6 generations F1 and F2 (Figure 15B), internal concentration  $C_i^*$  reaches its equilibrium value in less than three days, yielding a maximum stress intensity as early as hatching. When daphnids are not exposed during the embryonic stage, internal concentration  $C_i^*$  shows a much slower accumulation due to dilution by growth. Thus, the decrease in assimilation contributes to the difference in effect severity, only due to a difference in kinetics when exposure differs during the embryonic stage among generations. This occurs in experiments 4, 5 and 6 (Figure 15B) between generation F0 (not exposed during the embryonic stage) and generation F1 (exposed during the embryonic stage). The difference also explains why effects in generation F0 at a same exposure concentration are stronger when the embryonic stage is exposed (experiment 1 from Plaire *et al.*, 2013) than when it is not (experiment 4 from Massarin *et al.*, 2010). The decrease in assimilation does not contribute to the difference in effect severity as long as exposure during the embryonic stage does not differ among generations, like in experiments 1 and 2 generations F0 and F1 (Figure 15A) and in experiments 4 and 6 generations F1 and F2 (Figure 15B).
- Predicted curves for the damage level  $D^*$  shows a gradual accumulation and transmission of damage across generations. This second source of stress does not reach equilibrium value at the end of third exposed generation F2 (Figure 15B). As a consequence, inheritable damage appears as the true driving force for the transgenerational increase in effect severity observed from generations F0 to F2 (Massarin *et al.*, 2010) and even when exposure of the embryonic stage do not differ between generations F0 and F1 (Plaire *et al.*, 2013). Although damage level is reversible, its slow decrease after a return to uncontaminated medium in experiment 5 generation F1' and experiment 6 generation F2' (Figures 15B) makes the associated increase in costs for growth and maturation contributing the persistence of effects during recovery experiments 5 and 6.

#### 4.2.4.5 Estimated “toxicokinetic and toxicodynamic” parameters and implications

Values of “toxicokinetic and toxicodynamic” parameters obtained for the lowest least  $SSQ_{(tot)}$  are presented in Table 13. The value of no-effect concentration ( $NEC_1$ ) suggests that U-depl affects the digestive tract and assimilation only above  $5.3 \mu\text{g L}^{-1}$ . The value of no-effect damage level ( $NEC_2$ ) suggests that a transgenerational increase in costs for growth and maturation will occur at a concentration as low as  $0.04 \mu\text{g L}^{-1}$ , an untested exposure concentration which will unlikely differ from zero. This value implies that any level of molecular damage has a consequence for the energy budget, although the tiniest damage will cause a very slight non detectable change that organisms will cope with. The value of the uranium elimination rate  $k_e(0.33\text{day}^{-1})$  impacts the time required to reach equilibrium, within the duration of the embryonic stage, while the very low value of the reparation rate  $k_r(0.015\text{day}^{-1})$  reflects the slow transgenerational accumulation of damage. A final summary is given in Figure 16.

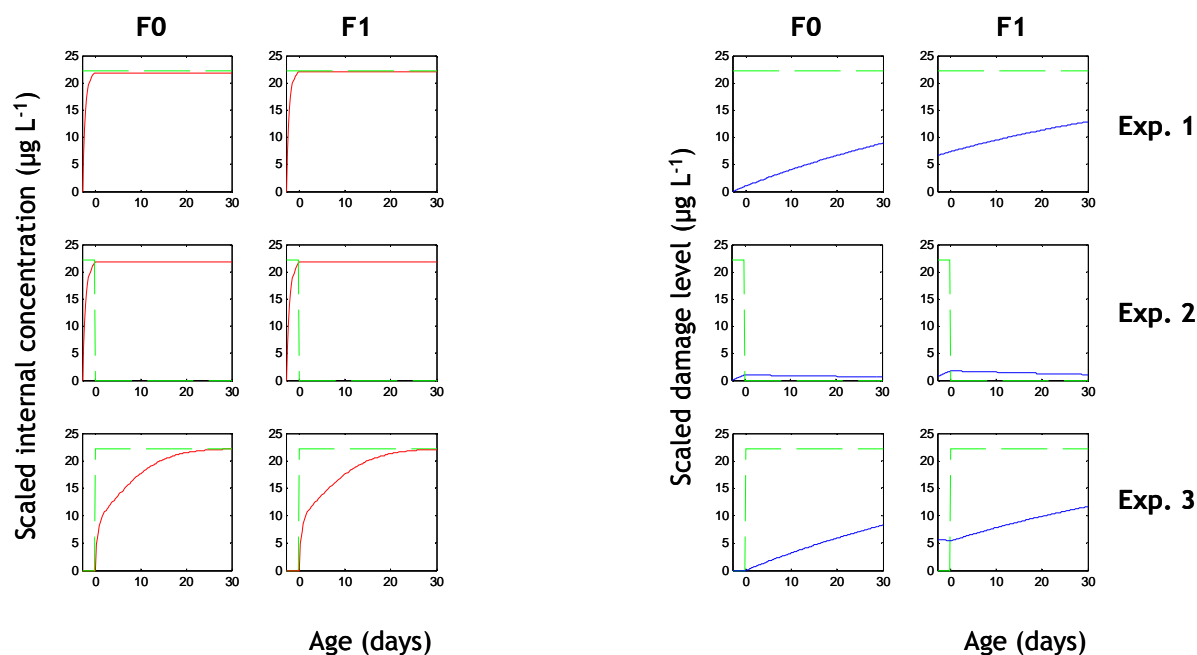


Figure 15A: Predicted curves for the stress factors, internal concentration  $C_i^*$  (causing an irreversible reduction in assimilation) and inheritable damage  $D^*$  (causing a reversible increase in costs for growth and maturation) in experiments 1 (continuous exposure to  $22.2 \mu\text{g L}^{-1}$ ), 2 (exposure to  $22.2 \mu\text{g L}^{-1}$  during the embryonic stage) and 3 (exposure to  $22.2 \mu\text{g L}^{-1}$  after hatching) from Plaire et al. (2013). Green dashed lines represent uranium exposure concentration  $C_e$ .

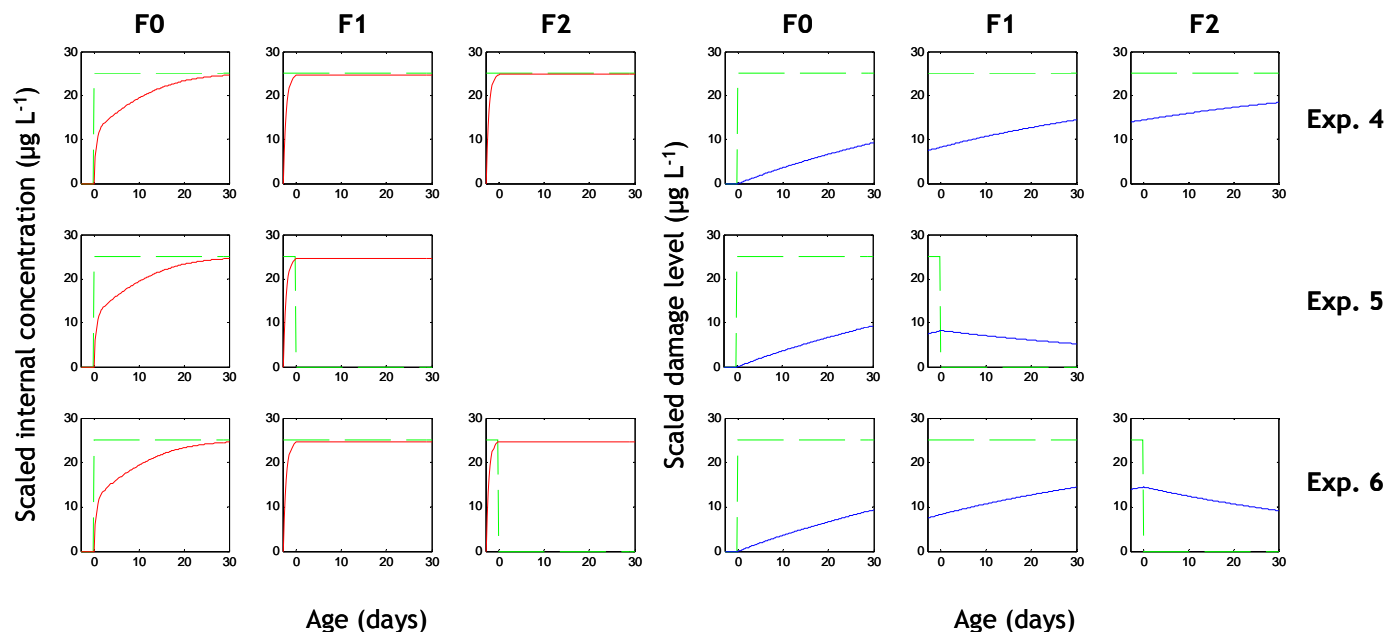


Figure 15B: Predicted curves for the stress factors, internal concentration  $C_i^*$  (causing an irreversible reduction in assimilation) and inheritable damage  $D^*$  (causing a reversible increase in costs for growth and maturation) in experiments 4 (continuous exposure to  $25 \mu\text{g L}^{-1}$ ), 5 (recovery from exposure to  $25 \mu\text{g L}^{-1}$  in generation F1') and 6 (recovery from exposure to  $25 \mu\text{g L}^{-1}$  in generation F2') from Massarin et al. (2010). Green dashed lines represent uranium exposure concentration  $C_e$ .

Table 13: “Toxicokinetic and toxicodynamic” parameters for the dual-stress DEB-tox model, estimated for all experiments and generations based on exposed datasets from Massarin et al. (2010) and Plaire et al. (2013).

Mode of action	Reduction in assimilation			Increase in costs for growth and maturation		
Stress factor	Internal concentration $C_i^*$			Damage $D^*$		
Parameter	$NEC_1$	$b_1$	$k_e$	$NEC_2$	$b_2$	$k_r$
Value	5.34 $\mu\text{g L}^{-1}$	0.003 $\text{L } \mu\text{g}^{-1}$	0.33 $\text{day}^{-1}$	0.04 $\mu\text{g L}^{-1}$	0.037 $\text{L } \mu\text{g}^{-1}$	0.015 $\text{day}^{-1}$

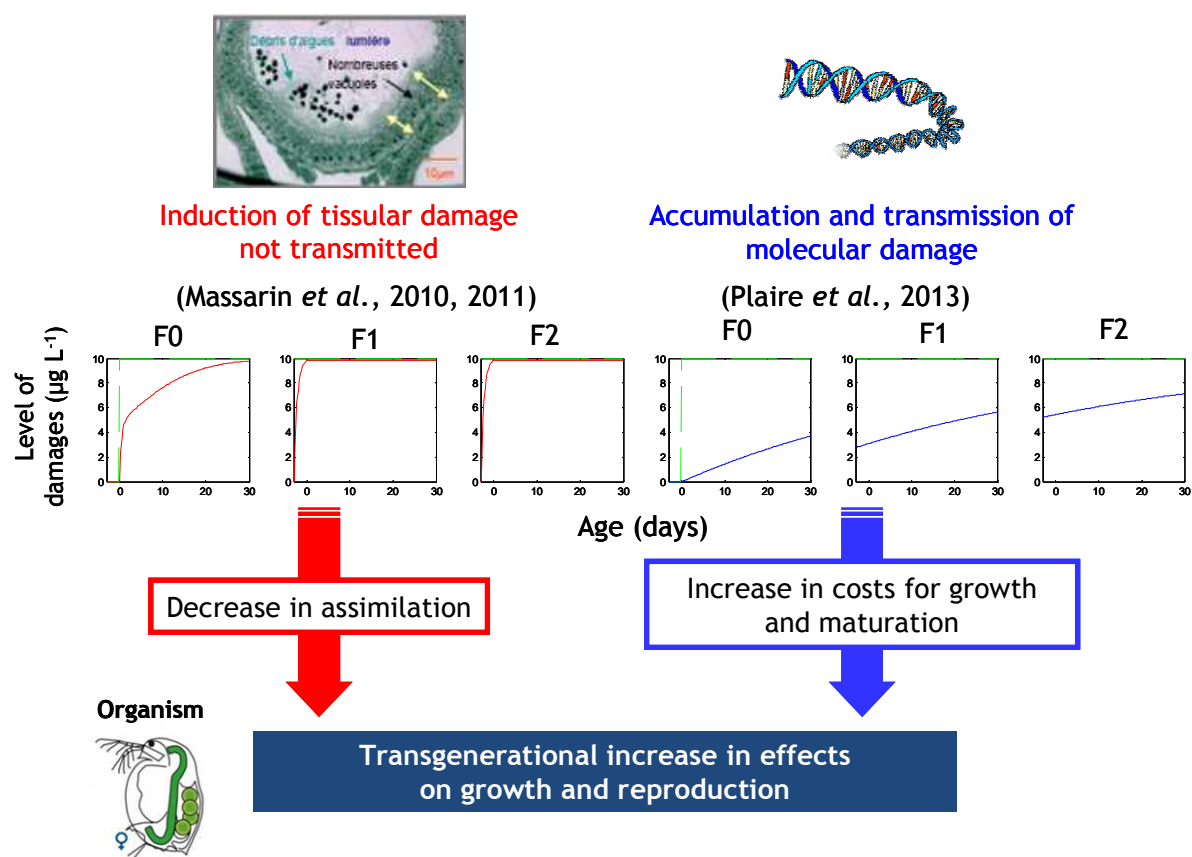


Figure 16: Contribution of a reduction in assimilation (induced by internalization of depleted uranium in red) and an increase in costs for growth and maturation (induced by a molecular damage accumulated across generations) to the transgenerational increase in effects on growth and reproduction, when daphnids are exposed to  $10 \mu\text{g L}^{-1}$  from hatching of generation F0 and over generations F1 and F2 (Massarin et al., 2010). Green dashed lines represent uranium exposure concentration, showing that embryonic stage is not exposed in generation F0.

### 4.3 Mechanistic comparison of gamma and alpha effects: identifying modes of actions and quantifying RBE

#### 4.3.1 Background

The daphnid *D. magna* is one of the few animal species for which *in vivo* effects data of chronic internal alpha and external gamma radiation are available (Alonzo *et al.*, 2006, 2008; Parisot *et al.*, in prep). These studies are achieved in the framework of the EC program ERICA for the alpha contamination experiments and of STAR for the gamma irradiation. Results which are presented in the STAR deliverable report 5.3. (November 2013) included survival, growth and reproduction data monitored in time for DEB-tox analyses. A multigenerational exposure over three successive generations to waterborne Am-241 (at average alpha dose rates from 0.3 to 15 mGyh<sup>-1</sup>) and to external Cs-137 gamma radiation (ranging from 0.007 to 35 mGyh<sup>-1</sup>) showed that an increase in effects on survival and reproduction occurs across generations under both alpha contamination and gamma irradiation. This increase is stronger under alpha exposure than under gamma exposure.

Using the same technique as Plaire *et al.* (2013), Parisot *et al.* (in prep) demonstrated that an accumulation and transmission of DNA alterations occurred over generations exposed to gamma radiation. DNA alterations measured using the RAPD-qPCR, were significant at a dose rate as low as 0.007 mGy h<sup>-1</sup>. This supported the assumption that increasing DNA alterations might be a good biomarker and/or the cause of the transgenerational increase in effects.

#### 4.3.2 Future directions

Relative biological effectiveness (*RBE*) will be compared with the DEB-tox approach using alpha and gamma radiation dataset acquired in *D. magna*, either comparing stress functions from two distinct fits between alpha and gamma or by fitting a common stress function for alpha and gamma with *RBE* as an extra parameter (Figure 17).

In order to properly account for the time course of alpha radiological stress, kinetics of internalized Am-241 and alpha dose rate need to be accurately described. As usual, a one compartment kinetic model with first order kinetics is used. Am-241 intake and elimination are proportional to body surface and, respectively, to exposure concentration  $C_e$  and internal concentration  $C_i$ :

$$\frac{dC_i}{dt} = C_e \frac{k_a}{l} - C_i \left( \frac{k_e}{l} + \frac{d}{dt} \ln l^3 \right)$$

with  $k_a$  and  $k_e$  the surface-specific accumulation and elimination rates (in time<sup>-1</sup>) and where the term  $\frac{d}{dt} \ln l^3$  corresponds to the dilution of Am-241 burden by growth. Unlike the simplified DEB-tox model, we chose here to use the value of  $C_i$  instead of the scaled internal concentration  $C_i^*$  because we need to calculate the actual alpha dose rate  $DR_\alpha$ . We are helped in this matter considering that Am-241 was accurately quantified in different compartments of daphnid body (Alonzo *et al.*, 2008). Kinetics of  $DR_\alpha$  can then be easily obtained using the

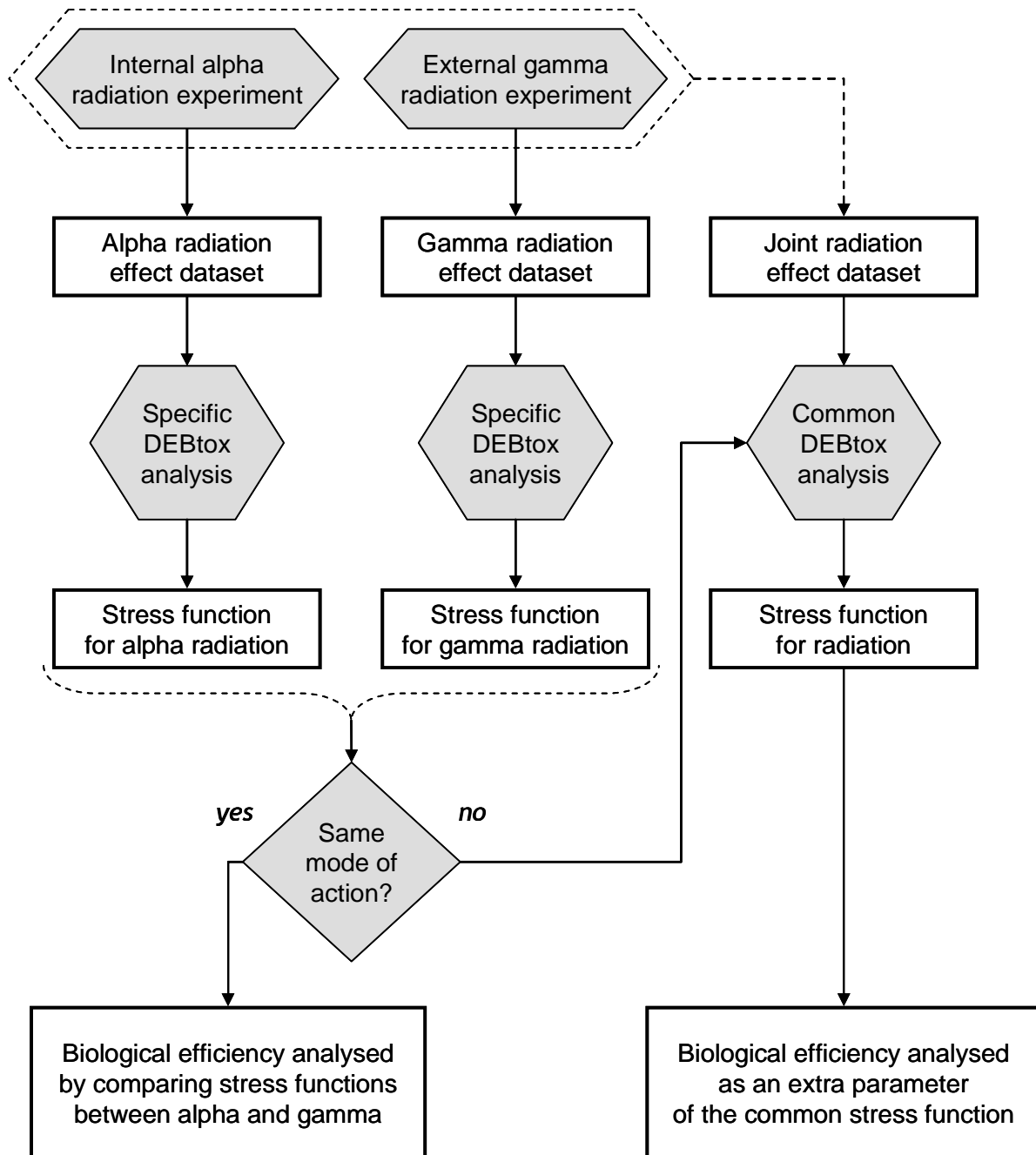


Figure 17. Suggested scheme for a mechanistic analysis of the biological efficiency of alpha and gamma radiation using DEB-tox.

dose conversion coefficients  $\alpha_{l,k}$  calculated for each body compartment  $k$  in a daphnid of size  $l$ .

$$\frac{dDR_{\alpha}}{dt} = \sum_k \frac{d(\alpha_{l,k} \cdot C_k)}{dt} = \sum_k \left( C_k \frac{d\alpha_{l,k}}{dt} + \alpha_{l,k} \frac{dC_k}{dt} \right) = \sum_k \left( C_k \frac{d\alpha_{l,k}}{dl} \cdot \frac{dl}{dt} + \alpha_{l,k} \frac{dC_k}{dt} \right)$$

where  $k$  includes internal tissues, cuticle and external medium.

On the other hand, the time course of the gamma radiological stress is most simple, considering that  $DR_{\gamma}$  is constant over time.

On this basis, biological perturbations induced by alpha and gamma radiation can be compared as dynamic processes. These will affect the energy budget of organisms through a stress function linked to 1)  $DR$  or 2) a scaled level of damage  $D^*$ :

$$1) \begin{cases} \sigma_x(DR_x) = 0 & \text{if } DR_x < NEDR_x \\ \sigma_x(DR_x) = b_x \cdot (DR_x - NEDR_x) & \text{if } DR_x \geq NEDR_x \end{cases}$$

or

$$2) \begin{cases} \sigma_x(D_x^*) = 0 & \text{if } D_x^* < NEDR_x \\ \sigma_x(D_x^*) = b_x \cdot (D_x^* - NEDR_x) & \text{if } D_x^* \geq NEDR_x \end{cases}$$

where  $\sigma_x$  is a stress function specific of a type  $x$  of radiation ( $x = \alpha$  or  $\gamma$ ) affecting the energy budget when the dose rate  $DR_x$  or the level of damage  $D_x^*$  exceeds a threshold value named the no-effect dose rate  $NEDR_x$  with  $b_x$  the slope of the effect intensity. The scaled damage level  $D_x^*$  has the units of a dose rate and follows a kinetics ruled by the equation:

$$\frac{dD_x^*}{dt} = k_{r,x} (DR_x - D_x^*)$$

with  $k_{r,x}$  the damage repair rate (in  $\text{time}^{-1}$ ), if a one-compartment model with first order kinetics is assumed again.

The radiological stress  $\sigma_x$  will affect the energy budget through one of the five standard DEB-tox modes of action. Two situations can arise:

- Identifying the same mode of action for alpha and gamma radiation will strongly suggest that radiological stress affects organisms through the same metabolic mechanism independent of the radiation type, making the comparison of the biological effectiveness between alpha and gamma radiation simple and straightforward (by a direct comparison of stress functions  $\sigma_{\alpha}$  and  $\sigma_{\gamma}$ ).

- Identifying different modes of action for alpha and gamma radiation will suggest that radiological stress may affect organisms through different metabolic mechanisms depending on the radiation type, and biological effectiveness of alpha and gamma radiation will be less comparable.

In both cases, one can nonetheless hypothesize that gamma and alpha radiation act through a unique mode of action. Under this assumption, identifying the most likely common mode of

action can be attempted, by fitting DEB-tox equations to both alpha and gamma radiation effect data with *RBE* concomitantly fitted as an extra parameter linking  $DR_\gamma$  and  $DR_\alpha$ :

$$DR_\alpha = RBE \cdot DR_\gamma$$

involved in the damage kinetics equation and in the stress function:

$$3) \begin{cases} \sigma(DR_x) = 0 & \text{if } DR_x < NEDR \\ \sigma(DR_x) = b \cdot (DR_x - NEDR) & \text{if } DR_x \geq NEDR \end{cases}$$

or

$$4) \begin{cases} \sigma(D^*) = 0 & \text{if } D^* < NEDR \\ \sigma(D^*) = b \cdot (D^* - NEDR) & \text{if } D^* \geq NEDR \end{cases}$$

where  $\sigma$  is a stress function common to any type  $x$  of radiation ( $x = \alpha$  or  $\gamma$ ) affecting the energy budget when the dose rate  $DR_x$  or the level of damage  $D^*$  exceeds a threshold value named the no-effect dose rate *NEDR* with  $b$  the slope of the effect intensity. The scaled damage level  $D^*$  has the units of a dose rate and follows a kinetics ruled by the equation:

$$\frac{dD^*}{dt} = k_r (DR_x - D^*)$$

with  $k_r$  the damage reparation rate (in  $\text{time}^{-1}$ ), if a one-compartment model with first order kinetics is assumed again.

## 5 *Lemna minor*

### 5.1 Introduction

To be able to parameterise a DEB-model for plants and to assess the effect of gamma and alpha radiation a number of experiments were established. As described in Deliverable 5.1 and 5.3, it was agreed upon that all partners would test gamma and alpha radiation. Alpha emitter americium-241 (Am-241) was chosen based on a number of criteria described in the deliverable 5.1 and 5.3. To set-up a dose response for Am-241 in *L. minor*, first the stability and availability of Am-241 was tested. Am-241 was added to different compositions growth media of *L. minor* including Steinberg medium (OECD, 2006), K-medium (Cedergreen et al., 2007), half strength Hunter medium (Brain and Solomon, 2007) and Hoagland medium (Vanhoudt et al., 2008) and the presence of the radionuclide after seven days in the filtered and unstirred medium was measured. In addition to the different standard media the composition of different cations, like Ca and Mg, was also altered in order to minimise Am-241 precipitation. However, Am-241 turned out to be unstable and precipitated in the different media tested so far. Hence the toxicity of this compound to *L. minor* could not be tested, and this in contrast to its effect on hydroponically grown *Arabidopsis* plants as reported in deliverable 5.3 (ref). The medium used for *Arabidopsis* plants was also tested but proved unsuitable for *L. minor*, probably due to a different experimental set-up used in *L.*

*minor* experiments (e.g. different experimental vessels and a much smaller medium volume to vessel area leading to Am-241 precipitating in the *L. minor* vessels). In conclusion, we were unable to test the effect of exposure to alpha radiation in *L. minor*. As an alternative a number of experiments were set up with uranium (U), also an alpha emitter but due to its low specific activity it has a higher chemical toxicity than radiological toxicity.

An overview of the experiments established to gather data to parameterise and validate a plant DEB-model is given in Table 16. Exposing plants to U is, in the facilities of SCK•CEN, easier than exposing them to external gamma radiation because we are dependent on another facility for the gamma source, with less flexibility to control light and temperature..

## 5.2 *The simplest DEB model for Lemna minor*

### 5.2.1 Purpose of the model

The beauty of DEB models lies in the fact that they can be used to investigate the interaction of stressors. These stressors could be toxicants such as radionuclides, radiation, or environmental variables such as light intensity, temperature, and nutrients. The model should thus be able to capture those environmental drivers that are essential for plants, which are light, temperature, and nutrients. The main challenge is to identify the essential model elements and to find a balance between model realism and model complexity (the latter can result in an over-parameterized model).

### 5.2.2 Modelling approach / Assumptions

The simplest DEB model for a plant, as suggested by Jager (personal communication), could be a model with only one reserve accounting for changes in either light or nutrients, under the assumption that the other is constant (see scheme Figure 18). Additionally, we account for only one structure, and thus model "biomass" as whole. The motivation for this assumption relies on the fact that the whole plant is in contact with the (contaminated) medium, and based on the observation that *L. minor* plants take up nutrients from both roots and shoots (Cedergreen and Madsen, 2002). Thus, accounting for roots and shoots separately in a radioecological context might not be necessary. Moreover, the standard OECD test protocol for *L. minor* does not prescribe measurement of the roots, but states that two growth measurements, fresh and/or dry weight and/or surface area shall be used for assessment of impacts on growth. The protocol is thus based on the hidden assumption that neither leaf thickness nor root/shoot ratio change, or that the change is minuscule so it does not play a role in the experimental results from toxicity studies. A full list of model assumptions is given in Table 14.

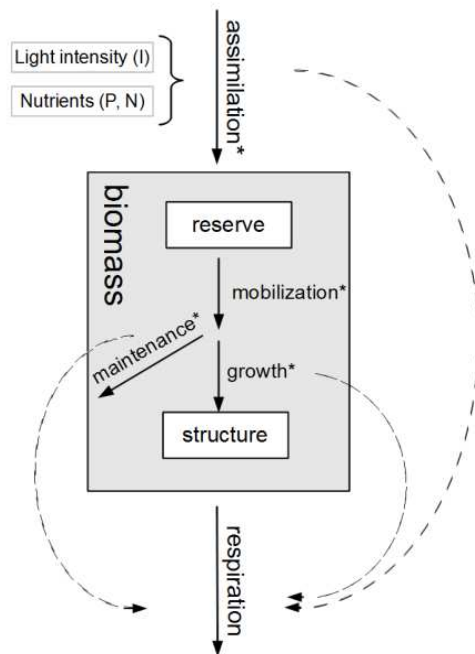


Figure 18: Schematic representation of the simple DEB-tox model for *L. minor*. Energy is first assimilated into reserves, and from there mobilized and allocated to growth and maintenance. All fluxes have contribution to respiration.

Table 14: List of assumptions underlying the simplest possible DEB model for *L. minor*

1. Surface area is growing proportional to volume (V1-morphy) → the entire plant colony can be regarded as an individual plant.
2. Only one of the essential energy components is limiting (light or a nutrient) → There are two types of biomass, structural volume and a single generalized reserve. Total biomass is the sum of the two.
3. Each structure has a constant composition (strong homeostasis, Kooijman, 2010) → a change in composition results from changes in the ratio of the two structures
4. Under constant conditions, the ratio of the two structures is constant, even when the plants grow (weak homeostasis)
5. Maximum assimilation rate is proportional to the surface area of the colony, and thus to its structural volume.
6. Assimilation into the reserves depends on light intensity or a nutrient through a hyperbolic relationship, while the other is assumed to be unlimiting.
7. Maintenance is proportional to structural volume and has priority over structural growth.
8. Only vegetative reproduction is considered. The investment into reproduction and maturation is ignored.
9. If the mobilisation from the reserve is not sufficient to pay maintenance costs, structure is used to pay these costs.

We can assume that *L. minor* plants grow in a way which is defined as V1-morphically in the DEB context: the surface area increases proportionally to the volume. As a proxy for volume, normally dry or wet weight is suitable. In V1-morphically growing organisms, the growth of an individual reflects the population growth rate, so the population growth can be modelled directly (Kooijman et al, 2002).

The change in structural volume  $V$  can be written out as

$$\frac{dV}{dt} = \left( \frac{[(\dot{k}_E + \dot{k}_M) e]}{e + g} - \dot{k}_M \right) \times V \quad \text{Eq. (E1)}$$

Where  $\dot{k}_E$  is the reserve turnover rate,  $\dot{k}_M$  the volume-specific maintenance rate,  $e$  is the reserve density, and  $g$  is the energy investment ratio, which gives an indication for the investment into growth. The model parameters and definitions are listed in Table 15.

Reserve density  $e$  is given as:

$$\frac{de}{dt} = \dot{k}_E(f - e) \quad \text{Eq. (E2)}$$

where  $f$  is the scaled functional response. In standard DEB for animals,  $f$  is defined as a function of food level. In the simplest DEB model for a plant, it could be defined as a function of light intensity. However, we hypothesize that the simplest model can be used for either (i) looking at constant nutrient concentrations, with varying light, or for looking at (ii) constant light conditions, where nutrient concentrations vary. In case (i),  $f$  would be defined as a function of light level, while in case (ii),  $f$  would be defined as a function of nutrient concentration. Both these assumptions need to be verified against data.

In DEB, toxic effects can normally be interpreted as changes in the parameter values that determine the allocation to the different metabolic functions. This means, if a compound appears to have an effect on maintenance, the parameter  $\dot{k}_M$  needs to be adapted to be able to capture the effect. As you can see from Eq. 1, the simplest model predicts exponential growth. All changes in DEB parameters lead to a change in exponential growth rate. Thus, it is impossible to distinguish between effects on growth, maintenance or reserve turnover rate. Although model testing has not yet been completed, it seems that this model might provide no additional informative beyond what can be learned from a simple model for exponential growth.

### 5.2.3 Possible extensions

A tree model has been suggested (Kooijman, 2010, chapter 5.3), but this model has never been parameterized (although pattern oriented model testing proved successful). This model has 8 state variables: two structures and three reserves per structure. It has more than double the number of parameters compared to the simplified model, which leads to immense data needs. It might be impossible to fully parameterize this model (personal communication with Kooijman). DEB models of lower complexity, which could serve as inspiration for plant

Table 15: Parameter definitions of the DEB model for *L. minor*

Parameter	Unit	Description	Definition
State variables			
$V$	$cm^3$	Structural volume	
$E$	$J$	Reserve	
$[E]$	$\frac{J}{cm^3}$	Reserve density	$[E] = \frac{E}{V}$
$e$	–	Scaled reserve density	$e = \frac{[E]}{[E_m]}$
Primary parameters			
$[E_m]$	$\frac{J}{cm^3}$	Maximum reserve density	
$[E_G]$	$\frac{J}{cm^3}$	Costs for growth	
$[\dot{\psi}_{Am}]$	$\frac{J}{cm^3 t}$	Assimilation efficiency	
$[\dot{\psi}_M]$	$\frac{J}{cm^3 t}$	Maintenance rate	
$X$	Concentration (i) or irradiance (ii), see main text	Nutrient (i) or light level (ii)	
$K$	Concentration (i) or irradiance (ii), see main text	Half saturation coefficient	
Compound parameters			
$k_M$	$t^{-1}$	Maintenance rate	$k_M = \frac{[\dot{\psi}_M]}{[E_G]}$
$k_E$	$t^{-1}$	Reserve turnover rate	$k_E = \frac{[\dot{\psi}_{Am}]}{[E_m]}$
$g$	–	Energy investment ratio	$g = \frac{[E_G]}{[E_m]}$
$f$	–	Scaled functional response	$f = \frac{X}{X + K}$

models, are for algae (Lorena et al, 2010), or for general photosynthesis (Muller, 2011). These models deal with multiple reserves, and they have been designed for V1-morphically growing organisms. These models could be tested and modified for use with *L. minor*, because we can assume that *L. minor* also grows V1-morphically (see above). Additional model compartments which might deserve consideration are additional structures: the root growth might respond to nutrient concentration and toxic stress (e.g. radiation). Modelling them

separately might be necessary in some scenarios, however, it would add a lot complexity and data needs.

### 5.3 Data needs for parameterization and verification

Extra growth describing data for *L. minor* are needed for two different purposes: (1) we need to verify our model assumptions, and (2) estimate parameter values. Can we neglect a differentiation between root and shoot compartments, or is it crucial? Do we need to account for multiple reserves, or can we capture the observed effect patterns with a model that only accounts for one reserve compartment?

To answer these questions, we have set up several experiments, some of which are still running, growing *L. minor* in varying light, temperature and nutrient conditions. Even in the simplest model, there is a need for experiments at different light levels (and nutrient levels) to be able to determine the reserve turnover parameter  $k_E$  (Kooijman et al, 2008).

*Lemna minor* is a well-established aquatic plant for ecotoxicological testing with standard endpoint parameters related to growth and photosynthesis e.g. chlorophyll a and b levels. For the experiments we used a 7-day growth inhibition test as described in OECD guideline 221(OECD, 2006) with some modifications. Phosphate concentrations were kept as low as possible due to the tendency of U to form precipitating complexes with phosphate, leading to changes in bioavailability and toxicity. Modifications were also made on the composition of the medium and variations in light and temperature as indicated in Table 16, to enable establishment of the temperature and light dependence of DEB-parameters.

Additionally, *L. minor* plants are kept in culture medium, and transferred into experimental medium for the duration of the experiments (for medium composition and method, Horemans et al., 2014). The reason is that when only using the experimental medium, the plants do not reach high growth rates as prescribed by the OECD guidelines. However, it was recently

Table 16: This table shows an overview of the experiments that were conducted for the parameterization of the DEB-tox model for *L. minor*. C: culture medium, E: experimental medium

Light →	normal light			high light			low light			day/ night
Temperature →	20	24	28	20	24	28	20	24	28	24
Controle	x	x	x	x	x	x	x	x	x	x
C→E										
C→C		x			x			x		
E→E		x			x			x		
Uranium	x	x	x	x	x	x	x	x	x	
Gamma		x								x

shown (Van Hoeck, SCK•CEN, unpublished data) that the ratio between root and shoot biomass changes substantially during the course of the one week experiment: from 10% root mass to 30% root mass. When following the OECD protocol, the roots are not measured separately. We thus conducted a number of experiments in which we cut the roots from the shoots, in different media combinations and under Uranium exposure, in order to determine the effect of the nutrient medium on *L. minor* growth and root/shoot ratio and the potential effect on the calculated ECX values.

#### **5.4 Effect of light, temperature and growth medium on *L. minor* growth, Uranium as a case study**

As indicated above, to establish a DEB-tox model for *L. minor*, characterisation of the main drivers of plant growth are needed. For gamma-experiments we were limited and could not vary temperature, and light conditions easily within the gamma irradiation facility. Therefore, it was chosen to perform the necessary experiments with U as a stressor. The laboratory for U experiments permitted us to also vary temperature and light. Uranium concentrations were chosen based on the dose-response curve set-up in WP4 (see MS report 47 of STAR and were kept below EC50 values

Different endpoints, such as frond number, frond growth, chlorophyll concentration and biomass accumulation were tested and growth inhibition was calculated as described in guideline 221 (OECD, 2006).

All experiments, as indicated in Table 16, have been conducted, but the analyses of the data are still on-going. However, the preliminary results indicate that light, temperature and medium each have a non-negligible effect on the U toxicity. As an example, we show growth inhibition, expressed per surface area, in an experiment where *L. minor* plants were exposed to 2.5, 5, 10 and 15  $\mu\text{M}$  of U at two different light levels. At the ‘normal’ light level (defined as within the range indicated by OECD guideline 221, we observed a stimulation in relative growth at the two lowest U concentrations, and growth inhibition thereafter (Figure 19). At the lower light level, there was a negligible stimulation in the lowest concentration, and growth inhibition in all other U concentrations. The ‘hormetic’ response was only visible at the higher light level. The analysis of measurements on photosynthetic-enzyme activity might give insight into the mechanisms behind these results.

#### **5.5 Gamma**

*L. minor* plants were exposed for seven days to different dose rates of gamma radiation, ranging from 0.1 mGy/h to 1.5 Gy/h. A significant dose dependent growth inhibition was observed after three days of exposure. After seven days, the maximum dose rates of gamma radiation achievable in our experimental set up (1.5 Gy/h) gave a growth inhibition of 62% (Figure 20). An EDR10 and EDR50 of  $\sim 80\text{mGy/h}$  and  $\sim 740\text{mGy/h}$  were estimated, respectively. In a recovery experiment in which irradiated plants were allowed to grow again for 7 days in control conditions it was shown that plant growth rate did not catch up with that of the non-irradiated group. On the contrary, plant cultures that showed a growth inhibition above 40% immediately after irradiation completely collapsed during the recovery period, indicating no recovery from the gamma induced damage (Figure 20). This resulted in a

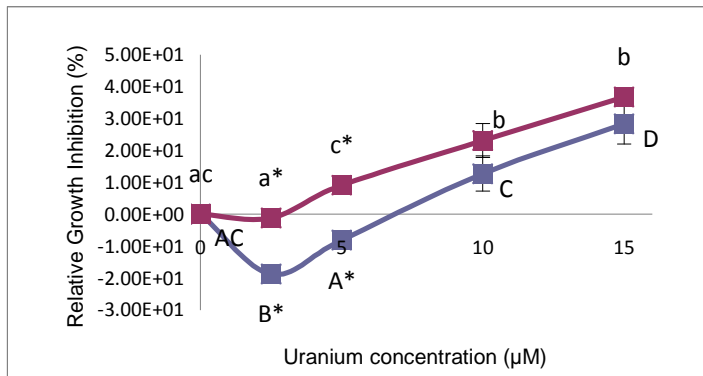


Figure 19: Growth inhibition observed in *L. minor* plants exposed to different levels of Uranium concentration for 7 days at two different light levels. The blue line corresponds to normal (OECD) light conditions ( $90 \pm 1 \mu E$ ), the red line corresponds to a lower light level ( $50 \pm 3 \mu E$ ). Small letters belong to the low light level, large letters to the normal light level. A different letter corresponds to a significant difference between levels of exposure within light level. A star corresponds to a significant difference between light levels. Data are mean values ( $n=3$  except for control where  $n = 6$ )  $\pm$  standard error.

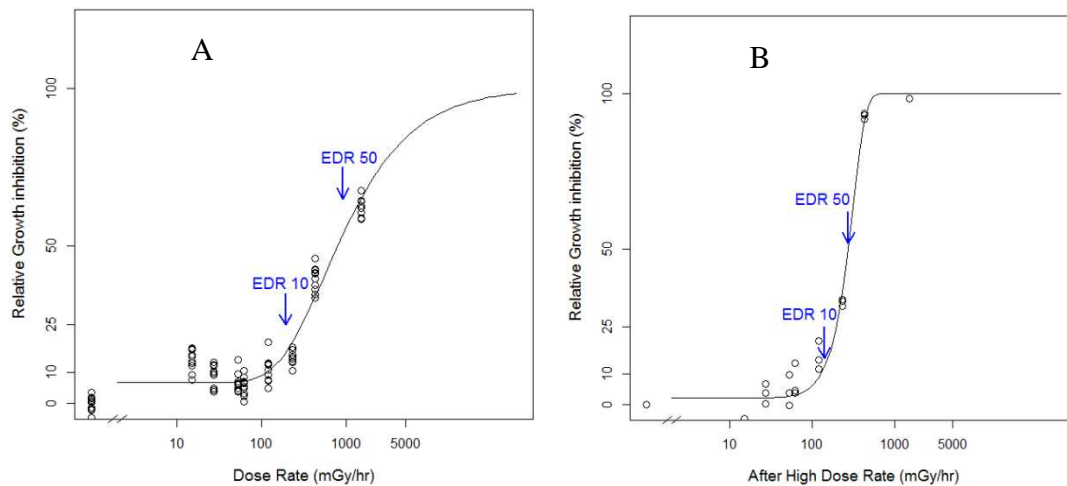


Figure 20: A: Growth inhibition observed in *L. minor* plants exposed to different dose rates of gamma irradiation ( $Cs-137$ ) for 7 days (5mM MES added). B: Growth inhibition observed in *L. minor* plants exposed to different gamma dose rates followed by a recovery period of 7days. For both figures data were fitted using drc package available in software “R” with a log-logistic function with 4 estimated parameters. ( $n=3$  except for controls receiving only natural background radiation where  $n=6$ )

steeper dose response curve, with an EDR10 that was unchanged but a EDR50 that was 3-fold lower. It thus seems that depending on the dose rate received, effects on *Lemna* plants differ with a change from survival to complete mortality. Future experiments with more intermediate dose rates and different plant species might indicate if growth is also dose-dependently affected and whether this phenomenon can be generalized to more plant species.

## 6 General conclusions and perspectives

Within the overarching objective of STAR's Work Package-5 being to enhance the scientific robustness of ecological protection criteria, we aimed to compare dose-response relationships and mode of action of effects induced under external gamma and internal alpha irradiation using a DEB-tox approach. We focussed on chronic exposure conditions, and included different model species *C. elegans*, *D. magna* and *L. minor*, as well as multigenerational studies. As described in STAR's Deliverable 5.1 and 5.3 alpha emitter americium-241 (Am-241) was chosen based on a number of criteria. Despite the effort so far we have been unable to test the effect of alpha exposures in *L. minor* due to experimental challenges of exposing Lemna plants to Am-241 (see Section 5). Additionally, due to a shutdown of laboratories at IRSN, we were not able to conduct further tests with *C. elegans* and Am-241. As an alternative, a number of experiments were set up with uranium, also an alpha emitter, but due to its low specific activity it has a higher chemical toxicity than radiological toxicity. Hence, a detailed comparison of the modes of action of alpha and gamma radiation within the DEB-tox context was not possible for *L. minor* or *C. elegans*. The relative biological effectiveness (*RBE*) can, however, be compared with the DEB-tox approach using alpha and gamma radiation dataset acquired in *D. magna*, either comparing stress functions from two distinct fits between alpha and gamma or by fitting a common stress function for alpha and gamma with *RBE* as an extra parameter as described in section 4.3.2.

Focusing only on the effect of gamma on *C. elegans* the DEB-tox analyses strongly suggested that under chronic exposure conditions two modes of action concomitantly affect the energy budget of nematodes. One of these modes of action is an increase in costs for growth and maturation and the other is a direct effect on reproduction. Radiological stress might be correlated to dose rate or to a level of damage cumulated during exposure. The fitted models underline a strong uncertainty which is due to individual variability and the fact that observed effects were relatively weak, even at the highest tested dose rate. Complementary knowledge would significantly help reducing this uncertainty and imply assessing a range of stronger effects (by testing stronger exposure dose rates, by increasing the duration of exposure so that effects over the same range of dose rates can become significant and/or by quantifying biomarkers which reflect the level of stress in nematodes).

A multigenerational study was set up in *D. magna*, though conducted with U-depl instead of Am-241. These showed that DNA alterations as measured by RAPD-qPCR might be a good biomarker of the inheritable damage causing the increase in sensitivity to depleted uranium across or the nature of the inheritable damage causing this increase. The DEB-tox analyses strongly suggest that the mode of action associated with the increase in effect severity across

generations is an increase in costs for growth and maturation, correlated to an inheritable and reversible damage level and that the non-heritable reduction in assimilation is irreversible and correlated to an internalized fraction of U-depl.. However, due to the very low activity of alpha radiation in U-depl., the effects described in this paragraph most likely originate from the chemical rather than radiological toxicity of U, and can thus not be used to extrapolate to other alpha emitters. Further experiments with Am-241 as originally intended will shed light on this.

In general, the DEB-tox analysis of the *C. elegans* and *D. magna* experiments shows its great potential for comparing effects of different stressors, especially radiation, on different species. However, it also shows the difficulties and uncertainties that still need to be resolved. Hypothesis testing is a powerful method that provides the option to compare between potential mechanisms. In the future, the benefits of additional measurements might be explored to more clearly identify the mechanistic mode of action in DEB. Currently, the DEB-tox analysis mainly serves as a tool that enables us to identify the areas that still need to be investigated in more detail, which is a great contribution and gives an invaluable addition to the value of the data gained during radioecological experiments.

As indicated, it was and is a challenge to use a DEB-tox approach for plants because previously there was no DEB model for a plant. Thus, the application of DEB-tox to *L. minor* takes more time than foreseen in the original plan. In the near future, we will scrutinize the performance of the simple DEB-tox model for *Lemna* and compare it to other available models (exponential growth, and the TKTD model by Schmitt et al, 2013). Further steps include setting up a more complex model (e.g. 2 reserves, 2-structures) and assessing the trade-off between added value of realism and complexity vs. usability.

In DEB theory, effects of stressors are interpreted as changes in parameter values. We expect that DNA damage caused by radiation will mainly increase the parameter maintenance costs ( $k_w$ ) in low doses, since the organisms can repair small amounts of DNA damage. Since radiation causes DNA damage both in animals (e.g. *D. magna*) and plants (e.g. *L. minor*), we can expect the same model parameter to be affected. At higher doses, the observed effects, however, changed. In *D. magna*, it seems that from a certain dose rate, the effects extend to additional costs on growth or reproduction. This phenomenon still needs to be explored for *Lemna* plants. We showed that once a certain dose rate is reached, *Lemna* plants can no longer recover from radiation exposure. There might be an intermediate dose rate, in which also first costs for growth are affected. DEB models provide the perfect stage for these types of comparisons between effect patterns and species.

## 7 References

- Adam, C., V. Larno, Giraudeau, M., Gania, Y., Bony, S., Devaux, A. (2006). Génotoxicité des radionucléides chez les organismes aquatiques : état de l'art et résultats préliminaires. ARET-Actualités. Association pour la Recherche en Toxicologie. Numéro spécial « Effets des toxiques chimiques / radioactifs sur le vivant », 103-118.
- Adam-Guillermin, C., S. Pereira, Della-Vedova, C., Hinton, T., Garnier-Laplace, J. (2012). Genotoxic and reprotoxic effects of tritium and external gamma irradiation on aquatic animals. Reviews on environmental contamination and toxicology, (220), 67-103.
- Alonzo, F., Gilbin, R., Bourrachot, S., Floriani, M., Morello, M., Garnier-Laplace, J. (2006) Effects of chronic internal alpha irradiation on physiology, growth and reproductive success of *Daphnia magna*. Aquatic Toxicology 80:228-236
- Alonzo, F., Gilbin, R., Zeman, F. A., Garnier-Laplace J. (2008) Increased effects of internal alpha irradiation in *Daphnia magna* after chronic exposure over three successive generations. Aquatic Toxicology, 87 (3) 146-156.
- Augustine, S., Gagnaire B., Adam-Guillermin, C., Kooijman, S. A. (2012) Effects of uranium on the metabolism of zebrafish, *Danio rerio*. Aquatic Toxicology, 118 9-26.
- Billoir, E., Delignette-Muller, L. M., Péry, A. R. R., Geffard, O., Charles, S. (2008) Statistical cautions when estimating DEB-tox parameters. Journal of Theoretical Biology, 254 (1) 55-64.
- Brain, R.A. and Solomon, K.R. (2007) A protocol for conducting 7-day daily renewal tests with *Lemna gibba*. Nature Protocols, 2(4), 979-987.
- Buisset-Goussen, A., Goussen, B., Della-Vedova, C., Galas, C., Adam-Guillermin, C., Lecomte-Pradines, C. (2014) Effects of chronic gamma irradiation: A multigenerational study using *Caenorhabditiselegans*. Journal of Environmental Radioactivity, in press.
- Byerly, L., Cassada, R. C., & Russell, R. L. (1976). The life cycle of the nematode *Caenorhabditis elegans*: I. Wild-type growth and reproduction. Developmental Biology, 51(1), 23-33
- Cedergreen, N., Abbaspoor, M., Sørensen, H., Streibig, J.C. (2007) Is mixture toxicity measured on a biomarker indicative of what happens on a population level? A study with *Lemna minor*. Ecotoxicology and Environmental Safety, 67(3), 323-332.
- Cedergreen, N. and Madsen, T. (2002) Nitrogen uptake by the floating macrophyte *Lemna minor*. New phytologist, 155, 285-292
- Gilbin, R., Alonzo, F., Garnier-Laplace, J. (2008) Effects of chronic external gamma irradiation on growth and reproductive success of *Daphnia magna*. Journal of Environmental Radioactivity, 99(1), 134-145.
- Goussen, B., Beaudouin, R., Dutilleul, M., Buisset-Goussen, A., Bonzom, J.-M., Péry, A. (in press) DEB-tox modelling applied to *Caenorhabditis elegans*: a case study on uranium.
- Hertel-Aas, T., Oughton, D.H., Jaworska, A., Bjerke, H., Salbu, B., Brunborg, G. (2007) Effects of Chronic Gamma Irradiation on Reproduction in the Earthworm *Eisenia fetida* (Oligochaeta). Radiation Research 168, 515-526
- Horemans, N., Van Hees, M., Van Hoeck, A., Saenen, E., De Meutter, T., Nauts, R., Blust, R., Vandenhove, H. (2014) Uranium and cadmium provoke different oxidative stress responses in *Lemna minor* L. Plant Biology, DOI: 10.1111/plb.12222
- Houtgraaf, J., Versmissen, J., van der Giessen, WJ (2006). A concise review of DNA damage checkpoints and repair in mammalian cells. Cardiovascular Revascularization Medicine (7), 165-172.

- ICRP, 2003. Relative Biological Effectiveness, Radiation Weighting and Quality Factor". ICRP Publication 92. Ann. ICRP 33 (4).
- Jager, T., Alda Álvarez, O., Kammenga, J. E., & Kooijman, S. A. L. M. (2005). Modelling nematode life cycles using dynamic energy budgets. *Functional Ecology*, 19(1), 136-144
- Jager, T., Albert, C., Preuss, T. G., Ashauer, R. (2011) General unified threshold model of survival - A toxicokinetic-toxicodynamic framework for ecotoxicology. *Environmental Science and Technology*, 45 (7) 2529-2540.
- Jager, T., Crommentuijn, T., van Gestel, C. A., Kooijman, S. A. (2007) Chronic exposure to chlorpyrifos reveals two modes of action in the springtail *Folsomia candida*. *Environmental Pollution*, 145 (2) 452-458.
- Jager, T., Crommentuijn, T., Van Gestel, C. A. M., Kooijman, S. A. L. M. (2004) Simultaneous modeling of multiple end points in life-cycle toxicity tests. *Environmental Science and Technology*, 38 (10) 2894-2900.
- Jager, T., Klok C. (2010) Extrapolating toxic effects on individuals to the population level: The role of dynamic energy budgets. *Philosophical Transactions of the Royal Society B: Biological Sciences*, 365 (1557) 3531-3540.
- Jager, T., Zimmer, E. I. (2012) Simplified Dynamic Energy Budget model for analysing ecotoxicity data. *Ecological Modelling*, 225 74-81.
- Jarvis, R. B., Knowles, J. F. (2003) DNA damage in zebrafish larvae induced by exposure to low-dose rate [gamma]-radiation: detection by the alkaline comet assay. *Mutation Research/Genetic Toxicology and Environmental Mutagenesis* 541(1-2): 63-69.
- Knight, C., Patel, M., Azevedo, R., & Leroi, A. (2002). A novel mode of ecdysozoan growth in *Caenorhabditis elegans*. *Evolution and Development*, 4(1), 16-27
- Knowles, J., Greenwood, L. (1994) The effects of chronic irradiation on the reproductive performance of *Ophryotrocha diadema* (polychaeta, dorvilleidae). *Marine Environmental Research* 38, 207-224
- Knowles, J., Greenwood, L. (1997) A comparison of the effects of long-term  $\beta$ - and  $\gamma$ -irradiation on the reproductive performance of a marine invertebrate *Ophryotrocha diadema* (Polychaeta, Dorvilleidae). *Journal of Environmental Radioactivity* 34, 1-7
- Knowles, J. F. (1999). Long-term irradiation of a marine fish, the plaice *Pleuronectes platessa*: an assessment of the effects on size and composition of the testes and of possible genotoxic changes in peripheral erythrocytes. *International Journal of Radiation Biology* 75(6): 773-782.
- Knowles, J. F. (2002). An investigation into the effects of chronic radiation on fish. Bristol, UK, Environment Agency.
- Kooijman, S., Metz, J. (1984) On the dynamics of chemically stressed populations: the deduction of population consequences from effects on individuals. *Ecotoxicology and Environmental Safety*, 8 (3) 254-274.
- Kooijman S. A. L. M., Bedaux J. J. M. (1996) Analysis of toxicity tests on *Daphnia* survival and reproduction. *Water Research*, 30 (7) 1711-1723.
- Kooijman, S.A.L.M. (2010) *Dynamic Energy Budget Theory for Metabolic Organisation*. Cambridge University Press, Cambridge
- Kooijman, S., Dijkstra, H., Kooi, B. (2002) Light-induced mass turnover in a mono-species community of mixotrophs. *Journal of Theoretical Biology*, 214, 233-254
- Kooijman, S.A.L.M., Sousa, T., Pecquerie, L., van der Meer, J., Jager, T. (2008) From food-dependent statistics to metabolic parameters, a practical guide to the use of dynamic energy budget theory. *Biological Reviews*, 83, 533-552
- Larsson, C.M. 2008. An overview of the ERICA Integrated Approach to the assessment and management of environmental risks from ionising contaminants. *J. Environ. Radioact.*, 99, 1364-1370.

- Lecomte-Pradines, C., Hertel-Aas, T., Coutris, C., Gilbin, R., Della-Vedova, C., Dubourg, N., Garnier-Laplace, J., Alonzo, F. (in preparation) First application of DEB-Tox model to the case of radiological toxicity: analysis of chronic external gamma radiation effects in *Caenorhabditis elegans*
- Lika, K., Nisbet, R. M. (2000) A dynamic energy budget model based on partitioning of net production. *Journal of Mathematical Biology*, 41 (4) 361-386.
- Lorena, A., Marques, G. M., Kooijman, S.A.L.M., Sousa, T. (2010) Stylized facts in microalgal growth: interpretation in a dynamic energy budget context. *Philosophical transactions of the royal society B-biological sciences*, 365, 3509-3521
- Martin, B. T., Zimmer, E. I., Grimm, V., Jager, T. (2011) Dynamic Energy Budget theory meets individual-based modelling: a generic and accessible implementation. *Methods in ecology and evolution*, 3(4), 445 - 449
- Massarin, S., Alonzo, F., Garcia-Sanchez, L., Gilbin, R., Garnier-Laplace, J., Poggiale, J. C. (2010) Effects of chronic uranium exposure on life history and physiology of *Daphnia magna* over three successive generations. *Aquatic Toxicology*, 99 (3) 309-319.
- Massarin, S., Beaudouin, R., Zeman, F., Floriani, M., Gilbin R., Alonzo, F., Pery, A. R. R. (2011) Biology-based modeling to analyze uranium toxicity data on *Daphnia magna* in a multigeneration study. *Environmental Science and Technology*, 45 (9) 4151-4158.
- Muller, E. B. (2011) Synthesizing units as modeling tool for photosynthesizing organisms with photoinhibition and nutrient limitation. *Ecological modelling*, 222, 637-644
- Nisbet, R. M., Muller, E. B., Lika, K., Kooijman, S. A. L. M. (2000) From molecules to ecosystems through dynamic energy budget models. *Journal of Animal Ecology*, 69 (6) 913-926.
- Noonburg, E., Nisbet, R., McCauley, E., Gurney, W., Murdoch, W., De Roos, A. (1998) Experimental testing of dynamic energy budget models. *Functional Ecology*, 12 (2) 211-222. .
- OECD. (2006) *Lemna* sp. growth inhibition tests. Guideline 221. Paris, France: Organisation for Economic Co-operation and Development.
- Parisot, F., Bourdineaud, J.P., Plaire, D., Garcia-Sanchez, L., Adam-Guillermin, C., Alonzo, F. (in preparation) Transgenerational study of molecular and organism-level mechanisms of gamma radiotoxicity in *Daphnia magna*.
- Pereira, S., Bourrachot, S., Cavalie, I., Plaire, D., Dutilleul, M., Gilbin, R., Adam-Guillermin, C. (2011) Genotoxicity of acute and chronic gamma-irradiation on zebrafish cells and consequences for embryo development. *Environmental Toxicology and Chemistry*, 30(12), 2831-2837.
- Plaire, D., Bourdineaud, J.P., Alonzo, A., Camilleri, V., Garcia-Sanchez, L., Adam-Guillermin, C., Alonzo, F. (2013) Transmission of DNA damage and increasing reprotoxic effects over two generations of *Daphnia magna* exposed to uranium. *Compar. Biochem. Physiol. C*, 158, 231-243
- Real, A., Sundell-Bergman, S., Knowles, J.F., Woodhead, D.S., Zinger, I. (2004) Effects of ionising radiation exposure on plants, fish and mammals: relevant data for environmental radiation protection. *Journal of Radiological Protection*, 24(4A), A123-A137.
- Sancar, A., Lindsey-Boltz, L.A., Ünsal-Kaçmaz, K., Linn, S. (2004). Molecular mechanisms of mammalian DNA repair and the DNA damage checkpoints. *Annual Review of Biochemistry* 73(1): 39-85.
- Schmitt, W.; Bruns, E.; Dollinger, M. & Sowig, P. (2013) Mechanistic TK/TD-model simulating the effect of growth inhibitors on *Lemna* populations. *Ecological Modelling*, 2013, 255, 1-10
- Simon, O., Massarin, S., Coppin, F., Hinton, T.G., Gilbin, R. (2011) Investigating the embryo/larval toxic and genotoxic effects of gamma irradiation on zebrafish eggs. *Journal of Environmental Radioactivity*, 102(11), 1039-1044.
- Smith, J.T., Willey, N.J., Hancock, J.T. (2012) Low dose ionizing radiation produces too few reactive oxygen species to directly affect antioxidant concentrations in cells. *Biology Letters*, 8(4), 594-597.

- Streffer, C. (2004) Effects of Ionising radiation in the low dose range - Radiobiological basis. In Current Trends in Radiation Protection (H. Metivier, L. Arranz, E. Gallego & A. Sugier, eds), E D P Sciences, Cedex A: pp 13-35.
- Swain, S., Wren, J. F., Stürzenbaum, S. R., Kille, P., Morgan, A. J., Jager, T., Jonker, M. J., Hankard, P. K., Svendsen, C., Owen, J., Hedley, B. A., Blaxter, M., Spurgeon, D. J. (2010) Linking toxicant physiological mode of action with induced gene expression changes in *Caenorhabditis elegans*. *BMC Systems Biology*, 4 1-19.
- Vandenhove, H., Vanhoudt, N., Wannijn, J., Hees, M.V., Cuypers, A. (2009) Effect of low-dose chronic gamma exposure on growth and oxidative stress related responses in *Arabidopsis thaliana*. *Radioprotection*, 44(5), 487-491.
- Vanhoudt, N., Vandenhove, H., Smeets, K., Remans, T., Van Hees, M., Wannijn, J., Vangronsveld, J., Cuypers, A. (2008) Effects of uranium and phosphate concentrations on oxidative stress related responses induced in *Arabidopsis thaliana*. *Plant Physiology and Biochemistry*, 46(11), 987-996.
- Williams, C (Ed.), 2004. Special Issue: Framework for assessment of environmental impact (FASSET) of ionising radiation in European ecosystems. *J. Radiological Protection* 24 (4A).
- Wren, J. F., Kille, P., Spurgeon, D. J., Swain, S., Sturzenbaum, S. R., Jager, T. (2011) Application of physiologically based modelling and transcriptomics to probe the systems toxicology of aldicarb for *caenorhabditis elegans* (Maupas 1900). *Ecotoxicology*, 20 (2) 397-408.
- Zimmer, E.I., Jager, T., Ducrot, V., Lagadic, L., Kooijman, SALM (2012) Juvenile food limitation in standardized tests: a warning to ecotoxicologists. *Ecotoxicology*, 21, 2195-2204